

# Electromagnetic form factors of singly heavy baryons in the self-consistent SU(3) chiral quark-soliton model

June-Young Kim<sup>1,\*</sup> and Hyun-Chul Kim<sup>1,2,†</sup>

<sup>1</sup>*Department of Physics, Inha University, Incheon 22212, Republic of Korea*

<sup>2</sup>*School of Physics, Korea Institute for Advanced Study (KIAS), Seoul 02455, Republic of Korea*

(Dated: November 22, 2021)

The self-consistent chiral quark-soliton model is a relativistic pion mean-field approach in the large  $N_c$  limit, which describes both light and heavy baryons on an equal footing. In the limit of the infinitely heavy mass of the heavy quark, a heavy baryon can be regarded as  $N_c - 1$  valence quarks bound by the pion mean fields, leaving the heavy quark as a color static source. The structure of the heavy baryon in this scheme is mainly governed by the light-quark degrees of freedom. Based on this framework, we evaluate the electromagnetic form factors of the lowest-lying heavy baryons. The rotational  $1/N_c$  and strange current quark mass corrections in linear order are considered. We discuss the electric charge and magnetic densities of heavy baryons in comparison with those of the nucleons. The results of the electric charge radii of the positive-charged heavy baryons show explicitly that the heavy baryon is a compact object. The electric form factors are presented. The form factor of  $\Sigma_c^{++}$  is compared with that from a lattice QCD. We also discuss the results of the magnetic form factors. The magnetic moments of the baryon sextet with spin 1/2 and the magnetic radii are compared with other works and the lattice data.

Keywords: Heavy baryons, electromagnetic form factors, pion mean fields, the chiral quark-soliton model

arXiv:1803.04069v2 [hep-ph] 1 Jun 2018

---

\* E-mail: junyoung.kim@inha.edu

† E-mail: hchkim@inha.ac.kr

## I. INTRODUCTION

A baryon can be viewed as  $N_c$  valence quarks bound by the meson mean field [1, 2] in the  $1/N_c$  expansion within quantum chromodynamics (QCD), where  $N_c$  denotes the number of colors. Witten showed explicitly in his seminal paper [1] that in two-dimensional QCD the baryon can be considered as a bound state of  $N_c$  valence quarks by the meson mean fields in the Hartree approximation. Since the mass of the nucleon is proportional to  $N_c$  and the meson-loop fluctuations are suppressed by  $1/N_c$ , such a mean-field approach is valid in the large  $N_c$  limit. The chiral quark-soliton model ( $\chi$ QSM) [3–6] was developed based on this idea. In the large  $N_c$  limit, the presence of the  $N_c$  valence quarks produces the chiral mean fields coming from the polarization of a Dirac sea that in turn influences self-consistently the valence quarks. In this picture, the baryon arises as a soliton that consists of the  $N_c$  valence quarks. A very important feature of the chiral mean field or the soliton is hedgehog symmetry. The  $\chi$ QSM described successfully various properties of the baryon octet and decuplet such as the electromagnetic (EM) properties [7–11], axial-vector form factors [12], tensor charges and form factors [13–18], semileptonic decays [19–21], parton distributions [22–24], and so on.

Very recently, it was shown that singly heavy baryons can be considered as  $N_c - 1$  valence quarks bound by the pion mean field [25], being motivated by Diakonov [26]. In the limit of the infinitely heavy quark mass ( $m_Q \rightarrow \infty$ ), the spin of the heavy quark  $\mathbf{J}_Q$  is conserved, which leads to the conservation of the spin of the light-quark degrees of freedom:  $\mathbf{J} = \mathbf{J}' - \mathbf{J}_Q$  [27, 28]. In this limit, the heavy quark inside a singly heavy baryon can be merely regarded as a static color source, which means that the heavy quark is required only to make the heavy baryon a color singlet. Thus, the flavor  $SU_f(3)$  representations of the lowest-lying heavy baryons are given by  $\mathbf{3} \otimes \mathbf{3} = \bar{\mathbf{3}} \oplus \mathbf{6}$ , of which the baryon antitriplet has  $J = 0$  and  $J' = 1/2$ , whereas the sextet has  $J = 1$ . The light quarks with  $J = 1$  being coupled to the spin of the heavy quark  $J_Q = 1/2$ , the baryon sextet have spins  $1/2$  and  $3/2$ . So, there are two representations with spin  $1/2$  and  $3/2$  in the baryon sextet, which are degenerate in the limit of  $m_Q \rightarrow \infty$ . The hyperfine spin-spin interaction will lift the degeneracy between these states with different spins [25].

In the  $\chi$ QSM, we can apply basically the same formalism on the singly heavy baryons, which have been developed for the description of light baryons. Considering the heavy quark as a static color source, the heavy baryon can be regarded as a system of the  $N_c - 1$  valence quarks with the heavy quark stripped off from the valence level. In the case of the light baryons, the collective Hamiltonian is constrained by the right hypercharge  $Y' = N_c/3$  imposed by the  $N_c$  valence quarks, which selects the lowest allowed  $SU_f(3)$  representations such as the octet ( $\mathbf{8}$ ) and the decuplet ( $\mathbf{10}$ ). However, when it comes to the singly heavy baryons, this constraint should be changed to be  $Y' = (N_c - 1)/3$  because of the  $N_c - 1$  valence quarks inside a heavy baryon and yields the antitriplet ( $\bar{\mathbf{3}}$ ) and the sextet ( $\mathbf{6}$ ) as the lowest allowed representations. In addition, we need to modify the valence parts of all moments of inertia and quark densities for the calculation of any form factors. This extension of the  $\chi$ QSM was rather successful in describing the masses of the lowest-lying singly heavy baryons in both the charmed and bottom sectors, and the mass of the  $\Omega_b^*$  was predicted [25, 29]. Moreover, newly found  $\Omega_c$  resonances [31] were well explained and classified. In particular, two of the  $\Omega_c$  resonances were interpreted as exotic baryons belonging to the antidecapentaplet ( $\bar{\mathbf{15}}$ ) with their narrow widths correctly reproduced [30, 32].

In the present work, we want to investigate the EM properties of the lowest-lying singly heavy baryons with spin  $1/2$ . Assuming that the mass of the heavy quark is infinitely heavy, we will show that the main features of the EM form factors are governed by the  $N_c - 1$  light quarks. Of course, the electric form factor requires a certain contribution from the heavy quark such that the charge of the heavy baryons should be correctly reproduced. Since the EM current is decomposed into the light and heavy parts, the heavy-quark contribution can be treated separately. Its effects on the electric form factors are just the constant ones within the present framework, which indicates that the heavy quark is considered to be a structureless particle. This is a natural consequence, because we deal with the heavy quark just as a static color source. Since any form factor in QCD should decrease rapidly as the square of the momentum transfer increases because of gluon exchanges between the quarks that constitutes a baryon, the present picture of the electric form factors may be put into question. However, keeping in mind that the  $\chi$ QSM is the low-energy effective theory of the nucleon, we still can treat the heavy quark as a static one in the limit of  $m_Q \rightarrow \infty$ , as far as the momentum transfer remains much smaller than the heavy-quark mass, i.e.,  $q^2 \ll m_Q^2$ . We will show that this approach indeed produces reasonable results for the electric form factors of the heavy baryons in comparison with the lattice data [33]. In the case of the magnetic form factors, the situation is even better. In the limit of  $m_Q \rightarrow \infty$ , the effects of the heavy quark vanishes, since the magnetic moment of the heavy quark is proportional to the inverse of the heavy-quark mass. Thus, the magnetic form factors of the singly heavy baryons are solely governed by the light quarks.

We sketch the structure of the present paper as follows: In Sec. II, we show how to compute the EM form factors of the heavy baryons within the  $\chi$ QSM. In Sec. III, we present and discuss the numerical results of the EM form factors and the corresponding charge and magnetic radii. We also examine the effects of the  $SU_f(3)$  symmetry breaking. The final section is devoted to the summary and conclusions.

## II. GENERAL FORMALISM

The EM current including the heavy quark (the charm quark or the bottom quark) is expressed as

$$J_\mu(x) = \bar{\psi}(x)\gamma_\mu\hat{Q}\psi(x) + e_Q\bar{\Psi}\gamma_\mu\Psi, \quad (1)$$

where  $\hat{Q}$  denotes the charge operator in  $SU_f(3)$ , defined by

$$\hat{Q} = \begin{pmatrix} \frac{2}{3} & 0 & 0 \\ 0 & -\frac{1}{3} & 0 \\ 0 & 0 & -\frac{1}{3} \end{pmatrix} = \frac{1}{2} \left( \lambda_3 + \frac{1}{\sqrt{3}}\lambda_8 \right). \quad (2)$$

Here,  $\lambda_3$  and  $\lambda_8$  are the flavor  $SU(3)$  Gell-Mann matrices. The  $e_Q$  in the second part of the EM current in Eq. (1) stands for the heavy-quark charge, which is given as  $e_c = 2/3$  for the charm quark or as  $e_b = -1/3$  for the bottom quark. Since the magnetic form factor of a heavy quark is proportional to the inverse of the corresponding heavy-quark mass, i.e.,  $\boldsymbol{\mu} \sim (e_Q/m_Q)\boldsymbol{\sigma}$ , we can ignore the contribution from the heavy quark current in the limit of  $m_Q \rightarrow \infty$ . However, we need to keep the second term in Eq. (1) when we compute the electric form factors. The EM form factors of the spin-1/2 baryons are defined by the matrix element of the EM current

$$\langle B, p' | J_\mu(0) | B, p \rangle = \bar{u}_B(p', \lambda') \left[ \gamma_\mu F_1(q^2) + i\sigma_{\mu\nu} \frac{q^\nu}{2M_N} F_2(q^2) \right] u_B(p, \lambda), \quad (3)$$

where  $M_N$  is the mass of the nucleon. The  $q^2$  stands for the four-momentum transfer  $q^2 = -Q^2$  with  $Q^2 > 0$ .  $u_B(p, \lambda)$  denotes the Dirac spinor with the momentum  $p$  and the helicity  $\lambda$ . The Dirac and Pauli form factors  $F_1(Q^2)$  and  $F_2(Q^2)$  can be written in terms of the Sachs EM form factors,  $G_E(Q^2)$  and  $G_M(Q^2)$

$$\begin{aligned} G_E^B(Q^2) &= F_1^B(Q^2) - \tau F_2^B(Q^2), \\ G_M^B(Q^2) &= F_1^B(Q^2) + F_2^B(Q^2), \end{aligned} \quad (4)$$

with  $\tau = Q^2/4M_N^2$ . In the Breit frame, the Sachs form factors are related to the time and space components of the EM current, respectively,

$$\begin{aligned} G_E^B(Q^2) &= \int \frac{d\Omega_q}{4\pi} \langle B, p' | J_0(0) | B, p \rangle, \\ G_M^B(Q^2) &= 3M_N \int \frac{d\Omega_q}{4\pi} \frac{q^i \epsilon_{ik3}}{i|\mathbf{q}|^2} \langle B, p' | J^k(0) | B, p \rangle. \end{aligned} \quad (5)$$

Thus, once we compute the matrix elements of the EM current, we can directly derive the EM form factors. Note that we consider the heavy-quark part separately.

The  $SU(3)$   $\chi$ QSM is characterized by the following low-energy effective partition function in Euclidean space

$$\mathcal{Z}_{\chi\text{QSM}} = \int \mathcal{D}\psi \mathcal{D}\psi^\dagger \mathcal{D}U \exp \left[ - \int d^4x \psi^\dagger iD(U)\psi \right] = \int \mathcal{D}U \exp(-S_{\text{eff}}), \quad (6)$$

where  $\psi$  and  $U$  represent the quark and pseudo-Nambu-Goldstone boson fields, respectively. The  $S_{\text{eff}}$  is the effective chiral action,

$$S_{\text{eff}}(U) = -N_c \text{Tr} \ln iD(U), \quad (7)$$

where  $\text{Tr}$  stands for the generic trace operator running over spacetime and all relevant internal spaces. The  $N_c$  is the number of colors, and  $D(U)$  the Dirac differential operator is defined by

$$D(U) = \gamma_4(i\partial - \hat{m} - MU\gamma_5) = -i\partial_4 + h(U) - \delta m, \quad (8)$$

where  $\partial_4$  denotes the Euclidean time derivative. We assume isospin symmetry, i.e.,  $m_u = m_d$ . We define the average mass of the up and down quarks by  $\bar{m} = (m_u + m_d)/2$ . Then, the matrix of the current quark masses is written as  $\hat{m} = \text{diag}(\bar{m}, \bar{m}, m_s) = \bar{m} + \delta m$ .  $\delta m$  is written as

$$\delta m = \frac{-\bar{m} + m_s}{3} \gamma_4 \mathbf{1} + \frac{\bar{m} - m_s}{\sqrt{3}} \gamma_4 \lambda^8 = M_1 \gamma_4 \mathbf{1} + M_8 \gamma_4 \lambda^8, \quad (9)$$

where  $M_1$  and  $M_8$  are the singlet and octet components of the current quark masses, expressed, respectively, as  $M_1 = (-\bar{m} + m_s)/3$  and  $M_8 = (\bar{m} - m_s)/\sqrt{3}$ . The SU(3) single-quark Hamiltonian  $h(U)$  is defined as

$$h(U) = i\gamma_4\gamma_i\partial_i - \gamma_4MU^{\gamma_5} - \gamma_4\bar{m}, \quad (10)$$

where  $U^{\gamma_5}$  represents the SU(3) chiral field. Since the hedgehog symmetry constrains the form of the classical pion field as  $\boldsymbol{\pi}(\mathbf{x}) = \hat{\mathbf{n}} \cdot \boldsymbol{\tau}P(r)$ , where  $P(r)$  is the profile function of the soliton, the SU(2) chiral field is written as

$$U_{\text{SU}(2)}^{\gamma_5} = \exp(i\gamma_5\hat{\mathbf{n}} \cdot \boldsymbol{\tau}P(r)) = \frac{1+\gamma_5}{2}U_{\text{SU}(2)} + \frac{1-\gamma_5}{2}U_{\text{SU}(2)}^\dagger \quad (11)$$

with  $U_{\text{SU}(2)} = \exp(i\hat{\mathbf{n}} \cdot \boldsymbol{\tau}P(r))$ . We now embed the SU(2) soliton into SU(3) by Witten's ansatz [2]

$$U^{\gamma_5}(x) = \begin{pmatrix} U_{\text{SU}(2)}^{\gamma_5}(x) & 0 \\ 0 & 1 \end{pmatrix}. \quad (12)$$

Since we consider the mean-field approximation, we can carry out the integration over  $U$  in Eq. (6) around the saddle point ( $\delta S_{\text{eff}}/\delta P(r) = 0$ ). This saddle-point approximation yields the equation of motion that can be solved self-consistently. The solution provides the self-consistent profile function  $P_c(r)$ .

The matrix elements of the EM current (3) can be computed within the  $\chi$ QSM by representing them in terms of the functional integral in Euclidean space,

$$\begin{aligned} \langle B, p' | J_\mu(0) | B, p \rangle &= \frac{1}{\mathcal{Z}} \lim_{T \rightarrow \infty} \exp\left(ip_4 \frac{T}{2} - ip'_4 \frac{T}{2}\right) \int d^3x d^3y \exp(-i\mathbf{p}' \cdot \mathbf{y} + i\mathbf{p} \cdot \mathbf{x}) \\ &\times \int \mathcal{D}U \int \mathcal{D}\psi \int \mathcal{D}\psi^\dagger J_B(\mathbf{y}, T/2) \psi^\dagger(0) \gamma_4 \gamma_\mu \hat{Q}\psi(0) J_B^\dagger(\mathbf{x}, -T/2) \exp\left[-\int d^4z \psi^\dagger iD(U)\psi\right], \end{aligned} \quad (13)$$

where the baryon states  $|B, p\rangle$  and  $\langle B, p'|$  are, respectively, defined by

$$\begin{aligned} |B, p\rangle &= \lim_{x_4 \rightarrow -\infty} \exp(ip_4 x_4) \frac{1}{\sqrt{\mathcal{Z}}} \int d^3x \exp(i\mathbf{p} \cdot \mathbf{x}) J_B^\dagger(\mathbf{x}, x_4) |0\rangle, \\ \langle B, p'| &= \lim_{y_4 \rightarrow \infty} \exp(-ip'_4 y_4) \frac{1}{\sqrt{\mathcal{Z}}} \int d^3y \exp(-i\mathbf{p}' \cdot \mathbf{y}) \langle 0 | J_B^\dagger(\mathbf{y}, y_4). \end{aligned} \quad (14)$$

The heavy baryon current  $J_B$  can be constructed from the  $N_c - 1$  valence quarks

$$J_B(x) = \frac{1}{(N_c - 1)!} \epsilon_{i_1 \dots i_{N_c-1}} \Gamma_{JJ_3 TT_3 Y}^{\alpha_1 \dots \alpha_{N_c-1}} \psi_{\alpha_1 i_1}(x) \dots \psi_{\alpha_{N_c-1} i_{N_c-1}}(x), \quad (15)$$

where  $\alpha_1 \dots \alpha_{N_c-1}$  represent spin-flavor indices and  $i_1 \dots i_{N_c-1}$  color indices. The matrices  $\Gamma_{JJ_3 TT_3 Y}^{\alpha_1 \dots \alpha_{N_c-1}}$  are taken to consider the quantum numbers  $JJ_3 TT_3 Y$  of the  $N_c - 1$  soliton. The creation operator  $J_B^\dagger$  can be constructed in a similar way. As for the detailed formalism of the zero-mode quantization and the techniques of computing the baryonic correlation function given in Eq. (13), we refer to Refs. [5, 7].

Having quantized the soliton, we obtain the collective Hamiltonian as

$$H_{\text{coll}} = H_{\text{sym}} + H_{\text{sb}}, \quad (16)$$

where

$$\begin{aligned} H_{\text{sym}} &= M_{\text{cl}} + \frac{1}{2I_1} \sum_{i=1}^3 J_i^2 + \frac{1}{2I_2} \sum_{p=4}^7 J_p^2, \\ H_{\text{sb}} &= \alpha D_{88}^{(8)} + \beta \hat{Y} + \frac{\gamma}{\sqrt{3}} \sum_{i=1}^3 D_{8i}^{(8)} \hat{J}_i. \end{aligned} \quad (17)$$

$I_1$  and  $I_2$  are the soliton moments of inertia. The parameters  $\alpha$ ,  $\beta$ , and  $\gamma$  for heavy baryons are defined by

$$\alpha = \left( -\frac{\bar{\Sigma}\pi N}{3m_0} + \frac{K_2}{I_2} \bar{Y} \right) m_s, \quad \beta = -\frac{K_2}{I_2} m_s, \quad \gamma = 2 \left( \frac{K_1}{I_1} - \frac{K_2}{I_2} \right) m_s, \quad (18)$$

where that the three parameters  $\alpha$ ,  $\beta$ , and  $\gamma$  are expressed in terms of the moments of inertia  $I_{1,2}$  and  $K_{1,2}$ . The valence parts of them are different from those in the light baryon sector by the color factor  $N_c - 1$  in place of  $N_c$ . The expression of  $\bar{\Sigma}_{\pi N}$  is similar to the  $\pi N$  sigma term again except for the  $N_c$  factor:  $\bar{\Sigma}_{\pi N} = (N_c - 1)N_c^{-1}\Sigma_{\pi N}$ . The detailed expressions for the moments of inertia and  $\bar{\Sigma}_{\pi N}$  are found in Ref. [29].

Because of the symmetry-breaking part of the collective Hamiltonian  $H_{sb}$ , the baryon wave functions are no more pure states but are mixed ones with those in higher SU(3) representations. Thus the wave functions for the baryon antitriplet ( $J = 0$ ) and the sextet ( $J = 1$ ) are derived, respectively, as [29]

$$\begin{aligned} |B_{\bar{\mathbf{3}}_0}\rangle &= |\bar{\mathbf{3}}_0, B\rangle + p_{\bar{\mathbf{15}}}^B |\bar{\mathbf{15}}_0, B\rangle, \\ |B_{\mathbf{6}_1}\rangle &= |\mathbf{6}_1, B\rangle + q_{\bar{\mathbf{15}}}^B |\bar{\mathbf{15}}_1, B\rangle + q_{\bar{\mathbf{24}}}^B |\bar{\mathbf{24}}_1, B\rangle, \end{aligned} \quad (19)$$

with the mixing coefficients

$$p_{\bar{\mathbf{15}}}^B = p_{\bar{\mathbf{15}}} \begin{bmatrix} -\sqrt{15}/10 \\ -3\sqrt{5}/20 \end{bmatrix}, \quad q_{\bar{\mathbf{15}}}^B = q_{\bar{\mathbf{15}}} \begin{bmatrix} \sqrt{5}/5 \\ \sqrt{30}/20 \\ 0 \end{bmatrix}, \quad q_{\bar{\mathbf{24}}}^B = q_{\bar{\mathbf{24}}} \begin{bmatrix} -\sqrt{10}/10 \\ -\sqrt{15}/10 \\ -\sqrt{15}/10 \end{bmatrix}, \quad (20)$$

respectively, in the basis  $[\Lambda_Q, \Xi_Q]$  for the antitriplet and  $[\Sigma_Q, \Xi'_Q, \Omega_Q]$  for the sextets. The parameters  $p_{\bar{\mathbf{15}}}$ ,  $q_{\bar{\mathbf{15}}}$ , and  $q_{\bar{\mathbf{24}}}$  are given by

$$p_{\bar{\mathbf{15}}} = \frac{3}{4\sqrt{3}}\alpha I_2, \quad q_{\bar{\mathbf{15}}} = -\frac{1}{\sqrt{2}}\left(\alpha + \frac{2}{3}\gamma\right) I_2, \quad q_{\bar{\mathbf{24}}} = \frac{4}{5\sqrt{10}}\left(\alpha - \frac{1}{3}\gamma\right) I_2. \quad (21)$$

Having obtained the mixing parameters, we are able to express explicitly the wave function of a state with flavor  $F = (Y, T, T_3)$  and spin  $S = (Y' = -2/3, J, J_3)$  in the representation  $\nu$  in terms of a tensor with two indices, i.e.,  $\psi_{(\nu; F), (\bar{\nu}; \bar{S})}$ , one running over the states  $F$  in the representation  $\nu$  and the other one over the states  $\bar{S}$  in the representation  $\bar{\nu}$ . Here,  $\bar{\nu}$  represents the complex conjugate of the  $\nu$ , and the complex conjugate of  $S$  is given as  $\bar{S} = (2/3, J, J_3)$ . Since a singly heavy baryon consists of  $N_c - 1$  light valence quarks, the constraint imposed on the right hypercharge should be modified from  $\bar{Y} = -Y' = N_c/3$  to  $\bar{Y} = (N_c - 1)/3$ . Thus, the collective wave function for the soliton with  $(N_c - 1)$  valence quarks is written as

$$\psi_{(\nu; F), (\bar{\nu}; \bar{S})}(R) = \sqrt{\dim(\nu)}(-1)^{Q_S} [D_{FS}^{(\nu)}(R)]^*, \quad (22)$$

where  $\dim(\nu)$  represents the dimension of the representation  $\nu$  and  $Q_S$  a charge corresponding to the baryon state  $S$ , i.e.,  $Q_S = J_3 + Y'/2$ .

The complete wave function for a heavy baryon can be constructed by coupling the soliton wave function to the heavy quark

$$\Psi_{B_Q}^{(\mathcal{R})}(R) = \sum_{J_3, J_{Q3}} C_{J, J_3, J_Q, J_{Q3}}^{J' J'_3} \chi_{J_{Q3}} \psi_{(\nu; Y, T, T_3), (\bar{\nu}; Y', J, J_3)}(R) \quad (23)$$

where  $\chi_{J_{Q3}}$  denote the Pauli spinors and  $C_{J, J_3, J_Q, J_{Q3}}^{J' J'_3}$  the Clebsch-Gordan coefficients.

The final expression for the electric form factor of a heavy baryon  $B$  can be written as

$$G_E^B(q^2) = \int d^3z j_0(|\mathbf{q}||\mathbf{z}|) \mathcal{G}_E^B(\mathbf{z}) + G_E^Q(q^2), \quad (24)$$

where the first part of Eq. (24) is the light-quark contribution to the electric form factor whereas the second part corresponds to the pointlike heavy quark. The electric charge density of a light-quark part can be expressed as

$$\begin{aligned} \mathcal{G}_E^B(\mathbf{z}) &= \frac{1}{\sqrt{3}} \langle D_{Q8}^{(8)} \rangle_B \mathcal{B}(\mathbf{z}) - \frac{2}{I_1} \langle D_{Qi}^{(8)} \hat{J}_i \rangle_B \mathcal{I}_1(\mathbf{z}) - \frac{2}{I_2} \langle D_{Qp}^{(8)} \hat{J}_p \rangle_B \mathcal{I}_2(\mathbf{z}) \\ &\quad - \frac{4M_8}{I_1} \langle D_{8i}^{(8)} D_{Qi}^{(8)} \rangle_B (I_1 \mathcal{K}_1(\mathbf{z}) - K_1 \mathcal{I}_1(\mathbf{z})) \\ &\quad - \frac{4M_8}{I_2} \langle D_{8p}^{(8)} D_{Qp}^{(8)} \rangle_B (I_2 \mathcal{K}_2(\mathbf{z}) - K_2 \mathcal{I}_2(\mathbf{z})) \\ &\quad - 2 \left( \frac{M_1}{\sqrt{3}} \langle D_{Q8}^{(8)} \rangle_B + \frac{M_8}{3} \langle D_{88}^{(8)} D_{Q8}^{(8)} \rangle_B \right) \mathcal{C}(\mathbf{z}), \end{aligned} \quad (25)$$

where the explicit expressions for the electric densities can be found in Refs. [7, 34] with the prefactors of the valence parts replaced by  $N_c - 1$ . The indices  $i$  and  $p$  are dummy ones running over  $i = 1, \dots, 3$  and  $p = 4, \dots, 7$ , respectively. In the present mean-field approach, the heavy-quark contribution to the electric form factor is just the constant charge of the corresponding heavy quark ( $e_c = 2/3$  or  $e_b = -1/3$ ), because the heavy quark is assumed to be a static color source and a pointlike particle. Of course, this is a rather crude approximation but it is still a reasonable one as far as we consider the electric form factors in low  $Q^2$  regions. Thus, we set  $G_E^Q(Q^2) = e_Q$  in the present work.

Since the integrations of the densities in Eq. (25) are given as

$$\int d^3z \mathcal{B}(\mathbf{z}) = N_c, \quad \frac{1}{I_i} \int d^3z \mathcal{I}_i(\mathbf{z}) = 1, \quad \frac{1}{K_i} \int d^3z \mathcal{K}_i(\mathbf{z}) = 1, \quad \int d^3z \mathcal{C}(\mathbf{z}) = 0, \quad (26)$$

and  $G_E^Q(0) = e_Q$ , the electric form factor  $G_E^B$  at  $Q^2 = 0$  turns out to be the charge of the corresponding heavy baryon.

The expression for the magnetic moment form factor of a baryon  $B$  is written as

$$G_M^B(q^2) = \frac{M_N}{|\mathbf{q}|} \int d^3z \frac{j_1(|\mathbf{q}||\mathbf{z}|)}{|\mathbf{z}|} \mathcal{G}_M^B(\mathbf{z}), \quad (27)$$

where the corresponding density of the magnetic form factors is given by

$$\begin{aligned} \mathcal{G}_M^B(\mathbf{z}) = & \langle D_{Q3}^{(8)} \rangle_B \left( \mathcal{Q}_0(\mathbf{z}) + \frac{1}{I_1} \mathcal{Q}_1(\mathbf{z}) \right) - \frac{1}{\sqrt{3}} \langle D_{Q8}^{(8)} J_3 \rangle_B \frac{1}{I_1} \mathcal{X}_1(\mathbf{z}) - \langle d_{pq3} D_{Qp}^{(8)} J_q \rangle_B \frac{1}{I_2} \mathcal{X}_2(\mathbf{z}) \\ & + \frac{2}{\sqrt{3}} M_8 \langle D_{83}^{(8)} D_{Q8}^{(8)} \rangle_B \left( \frac{K_1}{I_1} \mathcal{X}_1(\mathbf{z}) - \mathcal{M}_1(\mathbf{z}) \right) + 2M_8 \langle d_{pq3} D_{8p}^{(8)} D_{Qq}^{(8)} \rangle_B \left( \frac{K_2}{I_2} \mathcal{X}_2(\mathbf{z}) - \mathcal{M}_2(\mathbf{z}) \right) \\ & - 2 \left( M_1 \langle D_{Q3}^{(8)} \rangle_B + \frac{1}{\sqrt{3}} M_8 \langle D_{88}^{(8)} D_{Q3}^{(8)} \rangle_B \right) \mathcal{M}_0(\mathbf{z}). \end{aligned} \quad (28)$$

The indices  $p$  and  $q$  are the dummy indices running over  $4 \dots 7$ . The explicit forms for the magnetic densities can be found in Ref. [7, 34] with the prefactors of the valence parts replaced by  $N_c - 1$ . The matrix elements of the collective operators are explicitly given in Appendix A. The magnetic form factor at  $Q^2 = 0$  produces the magnetic moment of the corresponding baryon. So, it is convenient to express a collective operator for the magnetic moments [35] as

$$\begin{aligned} \hat{\mu} = & w_1 D_{Q3}^{(8)} + w_2 d_{pq3} D_{Qp}^{(8)} \cdot \hat{J}_q + \frac{w_3}{\sqrt{3}} D_{Q8}^{(8)} \hat{J}_3 \\ & + \frac{w_4}{\sqrt{3}} d_{pq3} D_{Qp}^{(8)} D_{8q}^{(8)} + w_5 \left( D_{Q3}^{(8)} D_{88}^{(8)} + D_{Q8}^{(8)} D_{83}^{(8)} \right) + w_6 \left( D_{Q3}^{(8)} D_{88}^{(8)} - D_{Q8}^{(8)} D_{83}^{(8)} \right), \end{aligned} \quad (29)$$

where the dynamical coefficients  $w_i$  can be found in Appendix B. The results of the magnetic moments and  $w_i$  are compared with those from the model-independent analysis [35] also in Appendix B.

### III. RESULTS AND DISCUSSION

We are now in a position to discuss the results from the present work. We first briefly mention how to fix the parameters of the model. We refer to Refs. [5, 7] for a detailed explanation of numerical methods. The only free parameter of the  $\chi$ QSM is the dynamical quark mass  $M$  of which the numerical value was already fixed by computing various form factors of the nucleon. Its most preferable value is  $M = 420$  MeV. Nevertheless, we have checked whether the present results are sensitive to it with  $M$  varied from 400 to 450 MeV. All the form factors presented in this work are rather insensitive to the value of  $M$ , so we choose the value for the best fit, i.e.,  $M = 420$  MeV as in the light-baryon sector case [5, 7, 12, 17, 18, 20]. Note that the same value of  $M$  was selected also for the mass splitting of the heavy baryons [29]. There are yet another parameters in the  $\chi$ QSM: the average mass of the current up and down quarks  $\bar{m}$ , the strange current quark mass  $m_s$ , and the cutoff parameter  $\Lambda$  of the proper-time regularization. The value of  $\bar{m}$  was fixed to be  $\bar{m} = 6.131$  MeV by reproducing the pion mass whereas the cutoff parameter is determined by reproducing the pion decay constant  $f_\pi = 93$  MeV.

The strange current quark mass can be in principle taken from its canonical value  $m_s = 150$  MeV which was obtained by reproducing the kaon mass in the model. However,  $m_s = 180$  MeV was used for the calculation of the form factors and other properties of the  $SU_f(3)$  light baryons effectively. Very recently, the dependence of the mass splittings of heavy baryons on  $m_s$  were examined within the same framework of the  $\chi$ QSM [29] and the best values of  $m_s$  were obtained to be  $m_s = 174$  MeV and  $m_s = 166$  MeV for the mass splittings of the charmed baryons and the bottom baryons, respectively. Thus, instead of using the previous value 180 MeV, we will use the same values of

$m_s$  as obtained in Ref. [29] for consistency, regarding  $m_s$  as an effective mass. However, the EM form factors of the heavy baryons show rather tiny dependence on the numerical value of  $m_s$ , so the difference of the  $m_s$  value does not affect the results at all.

### A. Electric form factors of the baryon antitriplet and sextet with spin 1/2

The electric form factor of a baryon at  $Q^2 = 0$  is the same as its corresponding charge. Integrating the electric charge density of the baryon given in Eq. (25) over three-dimensional space, one obtains the corresponding charge. In fact, the collective charge operator is found from Eq. (25):

$$\hat{Q} = \frac{N_c}{2\sqrt{3}}D_{38}^{(8)} + \frac{N_c}{6}D_{88}^{(8)} + \sum_{i=1}^7 D_{3i}^{(8)}\hat{T}_i + \frac{1}{\sqrt{3}}\sum_{i=1}^7 D_{8i}^{(8)}\hat{T}_i, \quad (30)$$

where  $\hat{T}_i$  are the generators of SU(3) group. Using the relations

$$\hat{T}_8 = \frac{N_c}{2\sqrt{3}}, \quad \hat{T}_3 = \sum_{i=1}^8 D_{3i}^{(8)}\hat{T}_i, \quad \hat{Y} = \frac{2}{\sqrt{3}}\sum_{i=1}^8 D_{8i}^{(8)}\hat{T}_i, \quad (31)$$

Then we find the well-known Gell-Mann-Nishijima formula in SU<sub>f</sub>(3)

$$\hat{Q} = \hat{T}_3 + \frac{\hat{Y}}{2}. \quad (32)$$

Sandwiching the charge operator  $\hat{Q}$  between the collective baryon wave functions, we get the charge of the light-quark pair inside the corresponding baryon. In order to yield the correct charge of the baryon concerned, we have to introduce in addition the charge of a heavy quark inside it, as mentioned previously already. Thus, the  $Q^2$  dependence of the electric form factor of a heavy baryon in the present scheme is solely governed by the light quarks. The contribution of the pointlike heavy quark is just its own constant charge  $e_Q$  as given in Eq. (24). Though this mean-field approximation may be a crude one, the  $Q^2$  dependence of the electric form factors will explain a certain characteristics of the electric structure of the heavy baryons.

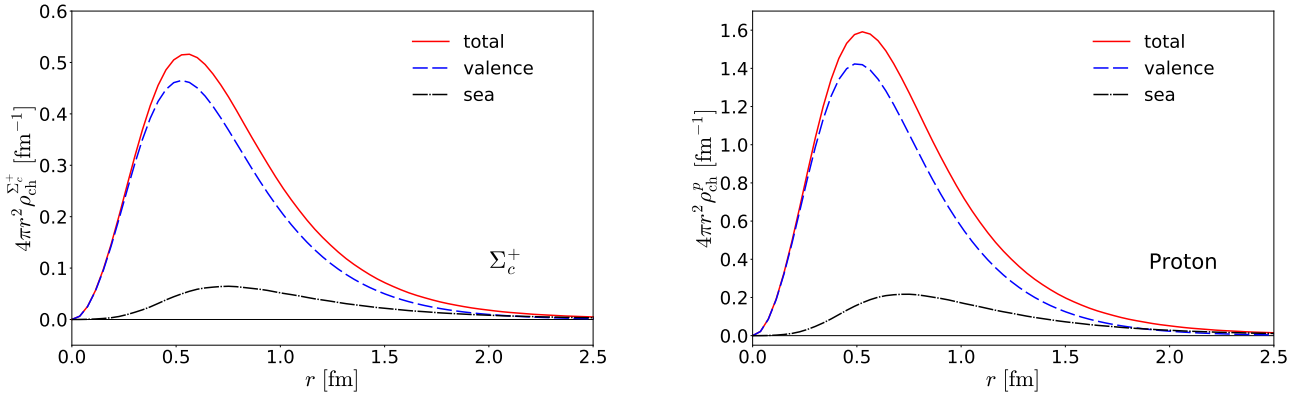


FIG. 1. Electric charge densities of the soliton ( $J = 1$ ) for the  $\Sigma_c^+$  soliton and the proton charge densities. In the left panel, the electric charge density of  $\Sigma_c^+$  is drawn whereas in the right panel that of the proton is depicted. The dashed curve represents the contribution of the valence quarks, while the dot-dashed one illustrates that of the sea quarks. The solid curve shows the total density.

In the present mean-field approach, the light-quark dynamics inside both a heavy baryon and a light baryon is treated on the same footing. Only difference lies in the different  $N_c$  counting factor, as explained previously. Thus, it is of great interest to examine the electric charge and magnetic densities of the heavy baryons with those of the proton and the neutron, before we compute the EM form factors of the heavy baryons. In the left panel of Fig. 1, we draw the electric charge densities of the soliton for  $\Sigma_c^+$ , which consists of the light-quark pair ( $ud$ ) with spin  $J = 1$ .

Note that  $\Sigma_c^+$  is a positive-charged member of the baryon antitriplet. The heavy quark inside  $\Sigma_c^+$  is assumed to be located at rest at the center of it. So, its charge density is just given by the delta function. The results are compared with those of the proton depicted in the right panel of Fig. 1. The general feature of the charge densities of the soliton of the light-quark pair inside  $\Sigma_c^+$  is almost the same as the proton one. The electric charge of the light-quark pair inside  $\Sigma_c^+$  is  $+1/3$  whereas the proton has  $+1$ . Thus, both the electric charge densities are positive definite over the whole  $r$  region. The difference between these two electric charge densities is found only in the strength of the electric charge. Hence, the proton electric charge density turns out to be approximately three times larger than that of the soliton for  $\Sigma_c^+$ . The sea-quark polarizations show marginal effects on both the electric charge densities.

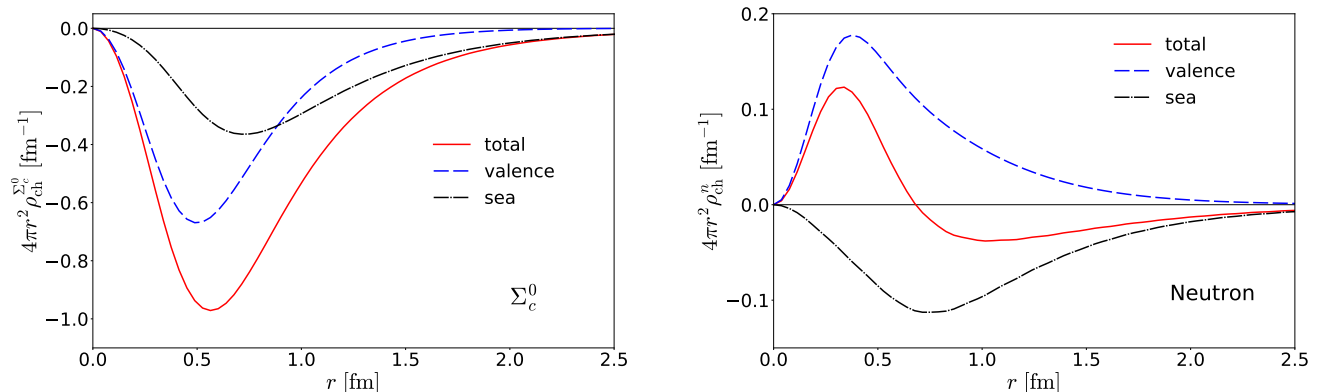


FIG. 2. Electric charge densities of the soliton ( $J = 1$ ) for  $\Sigma_c^0$  and the neutron charge densities. In the left panel, charge density of  $\Sigma_c^0$  is drawn whereas in the right panel that of the neutron is depicted. The dashed curve represents the contribution of the valence quarks, while the dot-dashed one illustrates that of the sea quarks. The solid curve shows the total contribution.

Figure 2 compares the electric charge densities of the soliton inside the neutral member  $\Sigma_c^0$  of the baryon antitriplet with those of the neutron ones. Since the  $\Sigma_c^0$  contains two down valence quarks, the charge distribution of the soliton inside  $\Sigma_c^0$  becomes negative. Apart from the sign of the densities, the general behavior of the light-quark electric charge density of  $\Sigma_c^0$  is very similar to that of the proton or  $\Sigma_c^+$ . The sea-quark polarization inside  $\Sigma_c^0$  is a stronger than those inside the  $\Sigma_c^+$  or proton case. On the other hand, the neutron electric charge density is rather different from that of  $\Sigma_c^0$ . In this case, the valence quarks govern the inner part of the neutron density, whereas the sea-quark polarization is dominant over its tail part. Thus even though the  $\Sigma_c^0$  is the neutral baryon, its light-quark charge density behave very differently, compared with the neutron density. We will soon see that this difference will be clearly shown in the electric form factors of the neutral heavy baryons. All other charge densities of the positive-charged heavy baryons are very similar to that of  $\Sigma_c^+$ , and those of the neutral ones to that of  $\Sigma_c^0$ .

In Fig. 3, the electric form factors of the singly positive-charged heavy baryons with spin  $1/2$  are drawn as functions of  $Q^2$ . They decrease monotonically as  $Q^2$  increases. This feature is very similar to that of the proton, which is already expected from the comparison of the charge densities in Fig. 1. So, it is also of great interest to compare the results of Fig. 3 with the proton electric form factor, as shown in Fig. 4. The electric form factor of the proton was obtained within the same framework with exactly the same parameters. The comparison exhibits a remarkable difference. The electric form factor of the proton falls off much faster than those of the singly positive-charged heavy baryons. It reveals a profound physical meaning: The heavy baryons are electrically compact objects, so that they are much smaller than the proton. This will be more clearly seen in the results of the charge radii which will be discussed later.

In Fig. 5, we show the results of the electric form factors of the neutral heavy baryons. They start to rise fast and then slow down as  $Q^2$  increases. The results are rather different from that of the neutron as discussed already in Fig. 2. The neutron electric form factor increases also as  $Q^2$  increases up to around  $0.4 \text{ GeV}^2$  and then starts to decrease very slowly [7, 36]. The experimental data also confirm this behavior of the neutron form factor [37]. As shown in Fig. 2, the neutron charge density is governed by the up quarks in the inner part of the neutron, whereas the negative-charged down quark dominates its tail part. On the other hand, the charge densities of the neutral heavy baryons are rather similar to those of the positive-charged ones except for the sign. Accordingly, the electric form factors of the neutral heavy baryons increase slowly and monotonically as  $Q^2$  increases. However, one should bear in mind that the present mean-field approach is only valid in the lower  $Q^2$  region, say, up to around  $1 \text{ GeV}^2$  or even lower values of  $Q^2$ .

In Fig. 6, we draw the numerical result of the electric form factor of  $\Sigma_c^{++}$ , comparing it with those from lattice



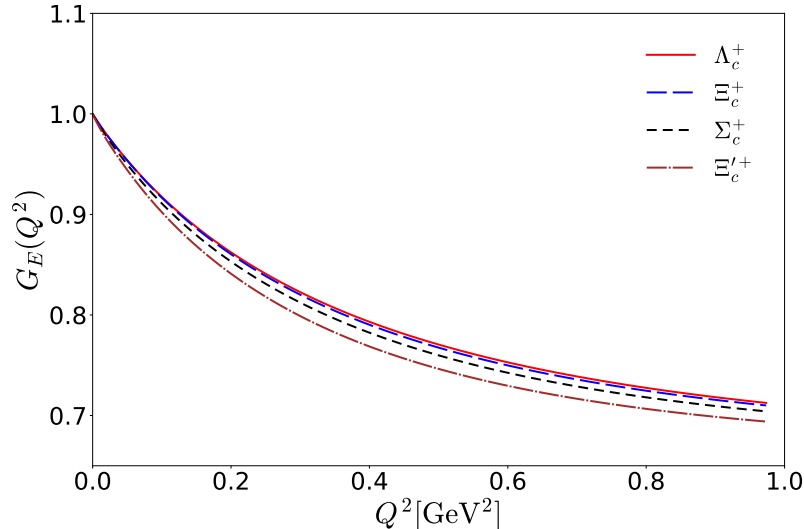


FIG. 3. Electric form factors of the singly positive-charged charmed baryons. The solid curve draws that of  $\Lambda_c^+$ , the long-dashed one for  $\Xi_c^+$ , the dashed one for  $\Sigma_c^+$ , and the dot-dashed one for  $\Xi_c'^+$ .

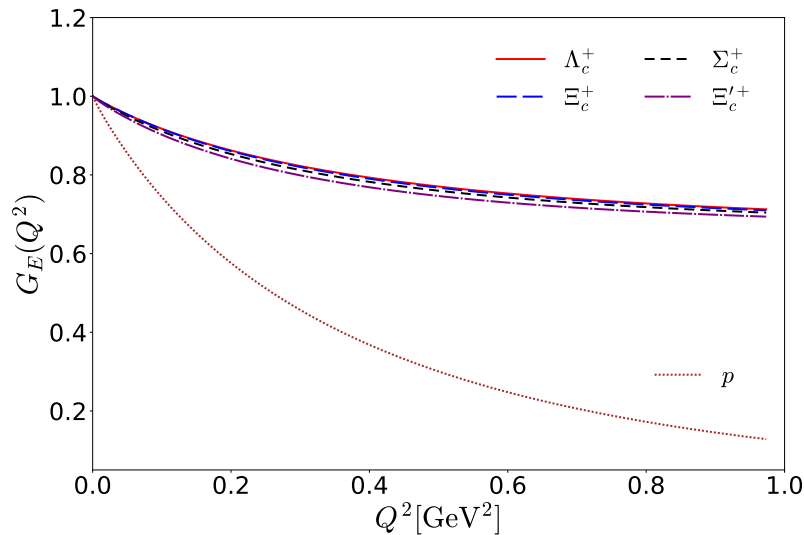


FIG. 4. Electric form factors of the singly positive-charged charmed baryons in comparison with that of the proton. The solid curve draws that of  $\Lambda_c^+$ , the long-dashed one for  $\Xi_c^+$ , the dashed one for  $\Sigma_c^+$ , and the dot-dashed one for  $\Xi_c'^+$ . The short-dashed curve depicts the proton electric form factor.

QCD [33]. Figure 6 shows that the present result falls off faster than the lattice ones. However, we want to emphasize on the fact that the lattice data on the electric form factor of the proton with the unphysical value of the pion mass tend to decrease slower than the experimental data. For example, all the lattice calculations [38–41] yield the results of the nucleon electric form factor, which fall off rather slowly in comparison with the experimental data. Even a very recent lattice calculation at the physical point [42] shows a similar feature. The same tendency was also found in the case of the tensor and anomalous tensor form factors of the nucleon [17, 18]. The lattice results of these form factors [43, 44] also fall off much more slowly than those results of the  $\chi$ QSM.

In the present mean-field approach, there is in principle no difference between the electric form factors of the charmed baryons and those of the bottom baryons, since the same light quarks govern the  $Q^2$  dependence of the form factors. The charge of the bottom quark makes their electric form factors distinguished from those of the charmed

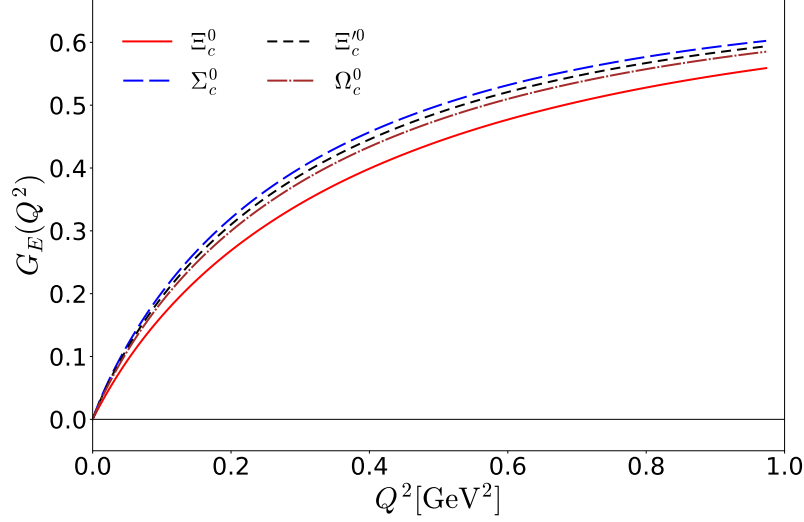


FIG. 5. Electric form factors of the neutral charmed baryons. The solid curve draws that of  $\Xi_c^0$ , the long-dashed one for  $\Sigma_c^0$ , the dashed one for  $\Xi_c'^0$ , and the dot-dashed one for  $\Omega_c^0$ .

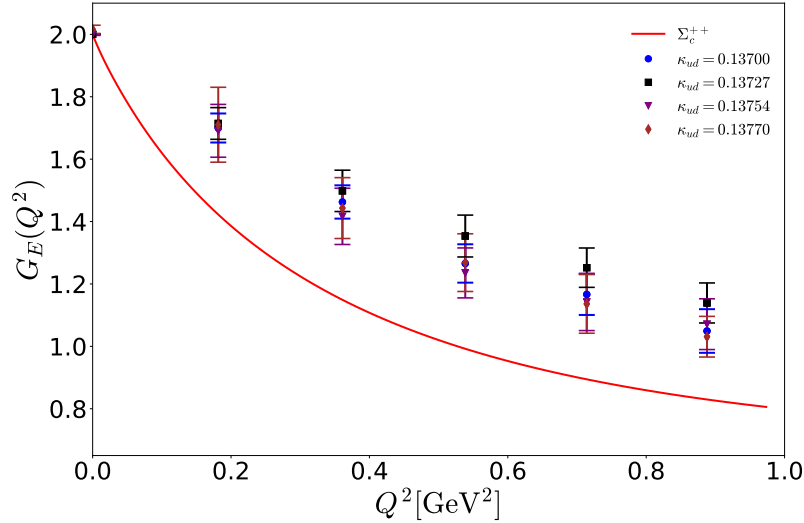


FIG. 6. Electric form factor of  $\Sigma_c^{++}$  as a function of  $Q^2$ . The result is compared with those from lattice QCD [33].  $k_{ud}$  denotes the light-quark hopping parameter [33].

baryons. In Fig. 7, we draw the electric form factors of the bottom baryons. In the upper left panel of Fig. 7, those of the neutral bottom baryons are depicted. Interestingly, they are all negative, which are different from those of the neutral charmed baryons. This can be understood from the different charges of the charm and bottom quarks. The upper right panel of Fig. 7 present the electric form factors of the negative-charged bottom baryons. That of  $\Sigma_b^+$  is illustrated in the lower panel of Fig. 7. We find that it becomes negative at around  $0.55 \text{ GeV}^2$ , which is again due to the negative charge  $e_b = -1/3$  of the bottom quark.

In the present approach, more important observables are the electric charge radii, since they are determined by the behavior of the electric form factors near  $Q^2 = 0$  and provide information on the sizes of the heavy baryons. The

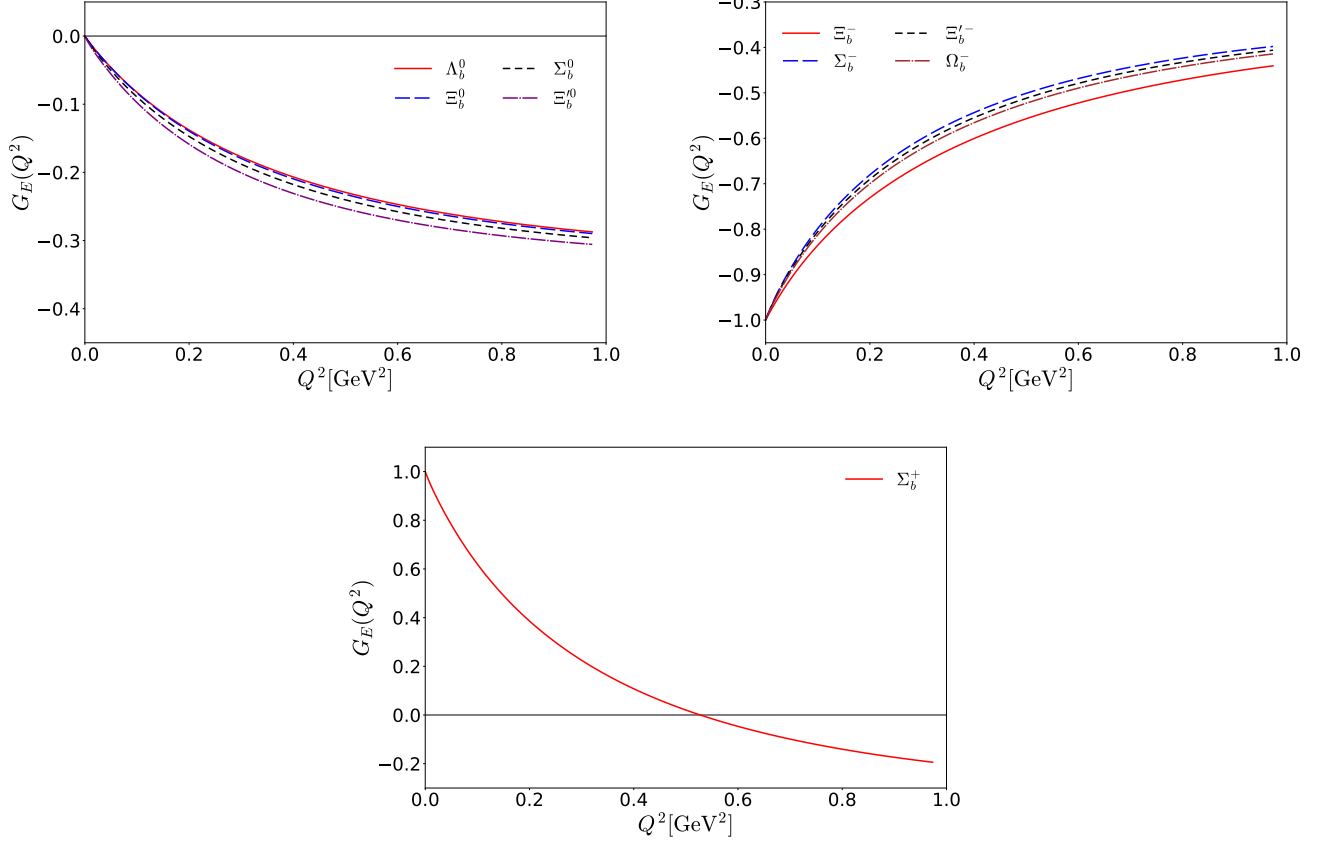


FIG. 7. Electric form factors of the bottom baryons as functions of  $Q^2$ . In the upper left panel, those of the neutral bottom baryons are drawn. The upper right panel presents those of the negative-charged bottom baryons. In the lower panel, that of  $\Sigma_b^+$  is drawn.

TABLE I. Electric charge radii of the charmed baryons in units of  $\text{fm}^2$ .

Baryon	$\langle r^2 \rangle_E^{B_c(m_s=0 \text{ MeV})}$	$\langle r^2 \rangle_E^{B_c(m_s=174 \text{ MeV})}$	[33]
$\Lambda_c^+$	0.26	0.24	–
$\Xi_c^+$	0.26	0.24	–
$\Xi_c^0$	-0.52	-0.51	–
$\Sigma_c^{++}$	0.60	0.59	$0.234 \pm 0.037$
$\Sigma_c^+$	0.30	0.27	–
$\Sigma_c^0$	-0.60	-0.66	–
$\Xi_c^{\prime+}$	0.30	0.30	–
$\Xi_c^{\prime0}$	-0.60	-0.63	–
$\Omega_c^0$	-0.60	-0.60	–

electric charge radii of the baryons is defined by

$$\langle r^2 \rangle_E^{B_Q} = -\frac{6}{G_E^B(0)} \left. \frac{dG_E^B(Q^2)}{dQ^2} \right|_{Q^2=0}. \quad (33)$$

Note that the electric charge radius given in Eq. (33) is normalized by the value of the corresponding electric form factor at  $Q^2 = 0$  for a charged heavy baryon. As for a neutral one, we do not normalize it. Since the heavy-quark contribution to the electric form factors is just the constant charge of the related heavy baryon, it does not contribute to the electric charge radii. Thus, the electric charge radii are solely determined by the solitons of the light-quark pair. In Table I, we list the results of the electric charge radii of the charmed baryons. In the second and third columns, those with  $m_s = 0$  and  $m_s = 174$  MeV are presented. The results show explicitly that in the  $\text{SU}_f(3)$  symmetric case

TABLE II. Electric charge radii of the bottom baryons in units of  $\text{fm}^2$ .

Baryon	$\langle r^2 \rangle_E^{B_b(m_s=0 \text{ MeV})}$	$\langle r^2 \rangle_E^{B_b(m_s=166 \text{ MeV})}$
$\Lambda_b^0$	0.26	0.24
$\Xi_b^0$	0.26	0.24
$\Xi_b^-$	0.52	0.51
$\Sigma_b^+$	0.60	0.60
$\Sigma_b^0$	0.30	0.27
$\Sigma_b^-$	0.60	0.66
$\Xi_b^{\prime 0}$	0.30	0.30
$\Xi_b^{\prime -}$	0.60	0.63
$\Omega_b^-$	0.60	0.60

the  $U$ -spin symmetry is preserved, i.e. we have the following relations in each representation

$$\begin{aligned}
\langle r^2 \rangle_E^{\Lambda_c^+} &= \langle r^2 \rangle_E^{\Xi_c^+} = -\frac{1}{2} \langle r^2 \rangle_E^{\Xi_c^0}, \\
\langle r^2 \rangle_E^{\Sigma_c^+} &= \langle r^2 \rangle_E^{\Xi_c^{\prime +}} = -\frac{1}{2} \langle r^2 \rangle_E^{\Sigma_c^0} - \frac{1}{2} \langle r^2 \rangle_E^{\Xi_c^{\prime 0}} = -\frac{1}{2} \langle r^2 \rangle_E^{\Omega_c^0} = \frac{1}{2} \langle r^2 \rangle_E^{\Sigma_c^{++}}.
\end{aligned} \tag{34}$$

The results listed in Table I indicate that the effects of  $\text{SU}_f(3)$  are marginal. We see that the baryon antitriplet have smaller sizes than those of the baryon sextet with spin 1/2. Moreover, as we already mentioned in discussion of Fig. 2, the electric charge radii of the positive-charged heavy baryons are noticeably smaller than that of the proton that is experimentally known to be  $\langle r^2 \rangle_E^p = (0.70 - 0.74) \text{ fm}^2$  [45]. The present result of the electric charge radius for  $\Sigma_c^{++}$  is compared with the lattice data [33]. As expected from Fig. 6, the present result is significantly larger than the lattice one. In Table II, we list the results of the electric charge radii of the bottom baryons. The results are the same as those of the charmed baryons in the present mean-field approach.

### B. Magnetic form factors of the baryon sextet with spin 1/2

We now turn our attention to the magnetic form factors of the heavy baryons, which are expressed in Eqs. (27) and (28). Assuming that the mass of the heavy quark is infinitely heavy, the heavy quark does not contribute to the magnetic form factors of the heavy baryons, since the heavy-quark contribution is proportional to the inverse of the heavy-quark mass ( $\mu_c \sim 1/m_Q$ ). Thus, the magnetic form factors of the heavy baryons are completely governed by the light-quark soliton. Note that in the present approach all the magnetic form factors of the baryon antitriplet vanish, since the soliton inside the baryon antitriplet has spin  $J = 0$ . It implies that they will be ascribed to higher-order corrections beyond the mean-field approximation and should be rather small. Thus, in this present work, we present the results of the magnetic form factors of the baryon sextet with spin 1/2. Those with spin 3/2 need to be treated separately, since their spin structures are more involved than the case of spin 1/2. The results of the spin 3/2 heavy baryons will appear elsewhere.

Figure 8 compares the magnetic densities of  $\Sigma_c^+$  with those of the proton. As in the case of the electric charge densities, we find that the general feature of the  $\Sigma_c^+$  magnetic densities is very similar to the proton ones. The difference is found only in the magnitudes of the densities. In Fig. 9, the magnetic densities of  $\Sigma_c^0$  are compared with those of the neutron. Both of them look similar each other except for the magnitudes again.

In the left panel of Fig. 10, we show the results of the magnetic form factors of the positive-charged baryon sextet with spin 1/2. The magnetic form factor of  $\Xi_c^{\prime +}$  is larger than that of  $\Sigma_c^+$ . Both form factors decrease monotonically as  $Q^2$  increases. In the right panel of Fig. 10, we compare the results of the magnetic form factors of  $\Sigma_c^+$  and  $\Xi_c^{\prime +}$  with that of the proton. We already expect that the proton magnetic form factor should be larger than those of these heavy baryons from the comparison of the magnetic densities in Fig. 8. In Figs. 11 and 12, we present the magnetic form factors of all the other members of the baryon sextet with spin 1/2. They start to fall off as  $Q^2$  increases. For completeness, we draw in Fig. 13 the results of the magnetic form factors of the bottom baryon sextet with spin 1/2.

As in the case of the electric charge radii, we also have the relation from the  $U$ -spin symmetry when  $m_s$  is set equal to zero:

$$\mu(\Sigma_c^0) = \mu(\Xi_c^{\prime 0}) = \mu(\Omega_c^0) = -2\mu(\Sigma_c^+) = -2\mu(\Xi_c^{\prime +}). \tag{35}$$

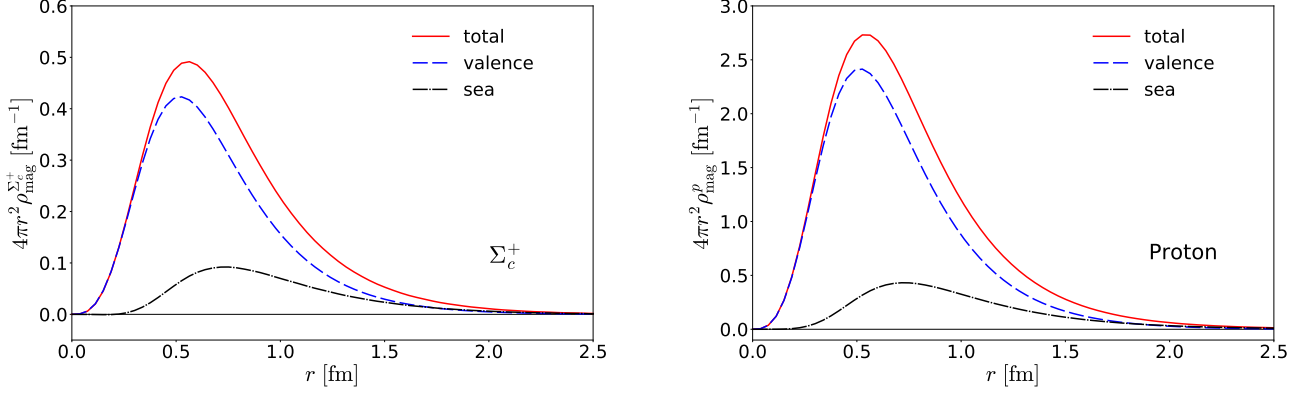


FIG. 8. Magnetic densities of the soliton ( $J = 1$ ) for the  $\Sigma_c^+$  and the proton magnetic densities. In the left panel, magnetic densities of  $\Sigma_c^+$  are drawn whereas in the right panel that of the proton are depicted. The dashed curve represents the contribution of the valence quarks, while the dot-dashed one illustrates that of the sea quarks. The solid curve shows the total contribution.

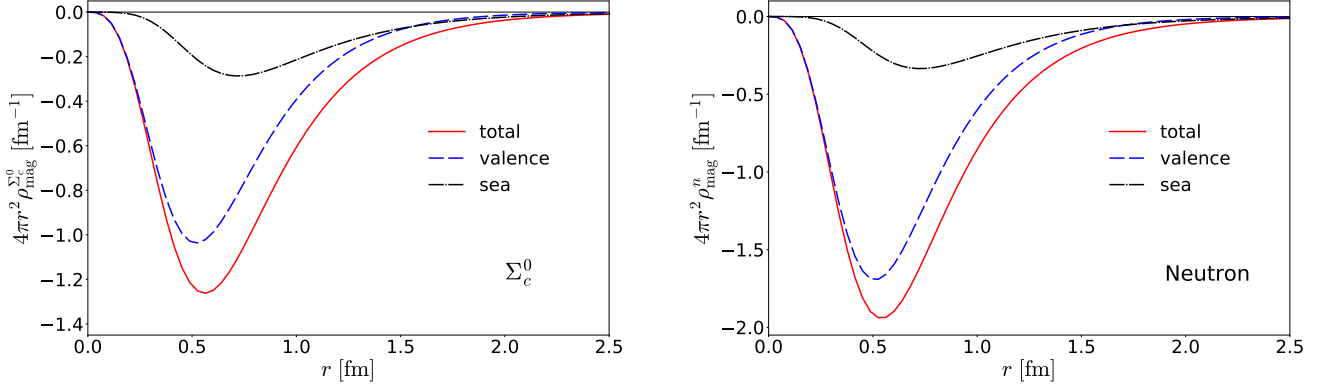


FIG. 9. Magnetic densities of the soliton ( $J = 1$ ) for the  $\Sigma_c^0$  and the neutron magnetic densities. In the left panel, magnetic density of  $\Sigma_c^0$  are drawn whereas in the right panel that of the neutron are depicted. The dashed curve represents the contribution of the valence quarks, while the dot-dashed one illustrates that of the sea quarks. The solid curve shows the total contribution.

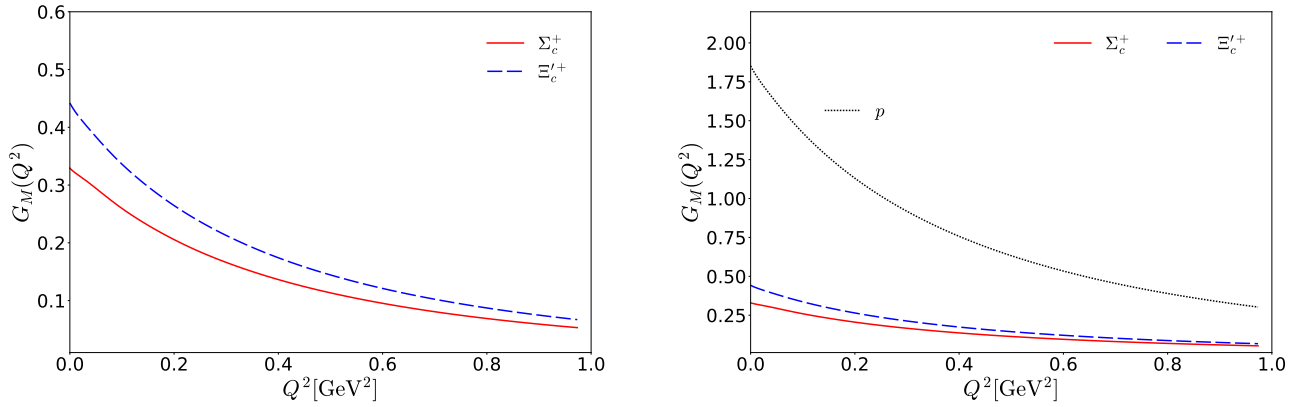


FIG. 10. Magnetic form factors of the singly positive-charged baryon sextet with  $J' = 1/2$ . In the left panel the magnetic form factors of the singly positive-charged baryon sextet are drawn. The solid curve depicts that of  $\Sigma_c^+$  whereas the dashed one illustrates that of  $\Xi_c'^+$ . In the right panel, the magnetic form factors of  $\Sigma_c^+$  and  $\Xi_c'^+$  are compared with that of the proton.

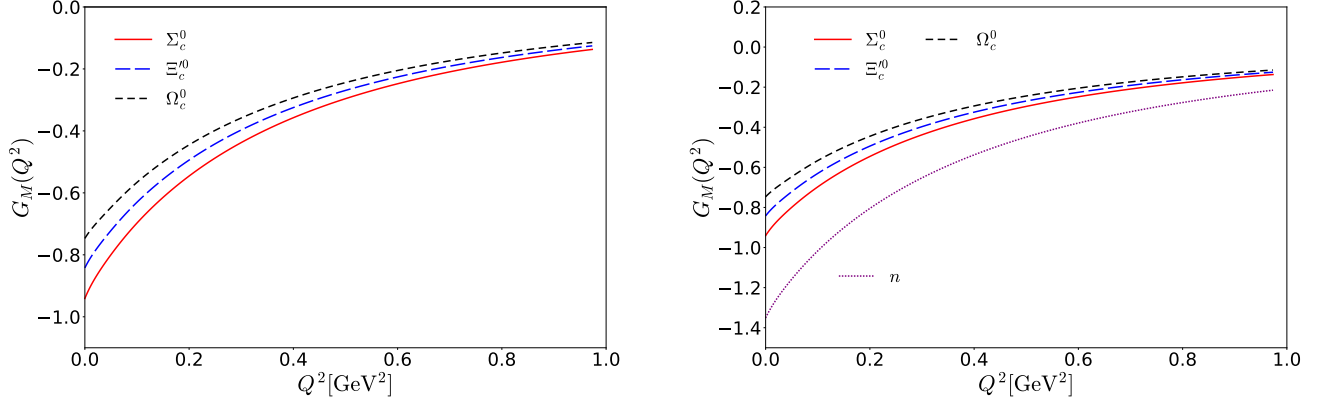


FIG. 11. Magnetic form factor of the neutral baryon sextet with  $J' = 1/2$ . In the left panel the magnetic form factors of the neutral baryon sextet are drawn. The solid curve depicts that of  $\Sigma_c^0$  whereas the dashed and short dashed ones illustrate those of  $\Xi_c'^0$  and  $\Omega_c^0$ , respectively. In the right panel, the magnetic form factors of the neutral baryon sextet are compared with that of the neutron.

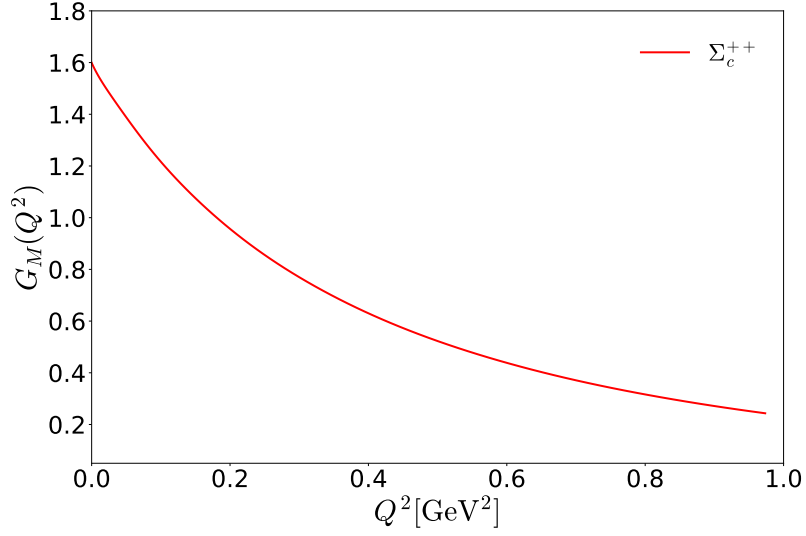


FIG. 12. Magnetic form factor of  $\Sigma_c^{++}$ .

As discussed in Ref. [35], we can find the relations arising from the isospin symmetry:

$$\begin{aligned}
 \mu(\Sigma_c^{++}) - \mu(\Sigma_c^+) &= \mu(\Sigma_c^+) - \mu(\Sigma_c^0), \\
 \mu(\Sigma_c^0) - \mu(\Xi_c'^0) &= \mu(\Xi_c'^0) - \mu(\Omega_c^0), \\
 2[\mu(\Sigma_c^+) - \mu(\Xi_c'^0)] &= \mu(\Sigma_c^{++}) - \mu(\Omega_c^0).
 \end{aligned} \tag{36}$$

Note that relations in Eq. (36) are also valid when the  $SU_f(3)$  symmetry is broken. Yet another interesting relation is the sum rule of the baryon magnetic moments of the baryon sextet with spin 1/2. If one adds all the magnetic moments of the baryon sextet with spin 1/2 in the  $SU_f(3)$  symmetric case, then we obtain the sum rule

$$\sum_{B_c \in \text{sextet}} \mu(B_c) = 0. \tag{37}$$

In Ref. [10], one finds a very similar relation for the magnetic moments of the baryon decuplet. However, while the sum of all the magnetic moments of the baryon decuplet is the same as that of all the electric charges of the

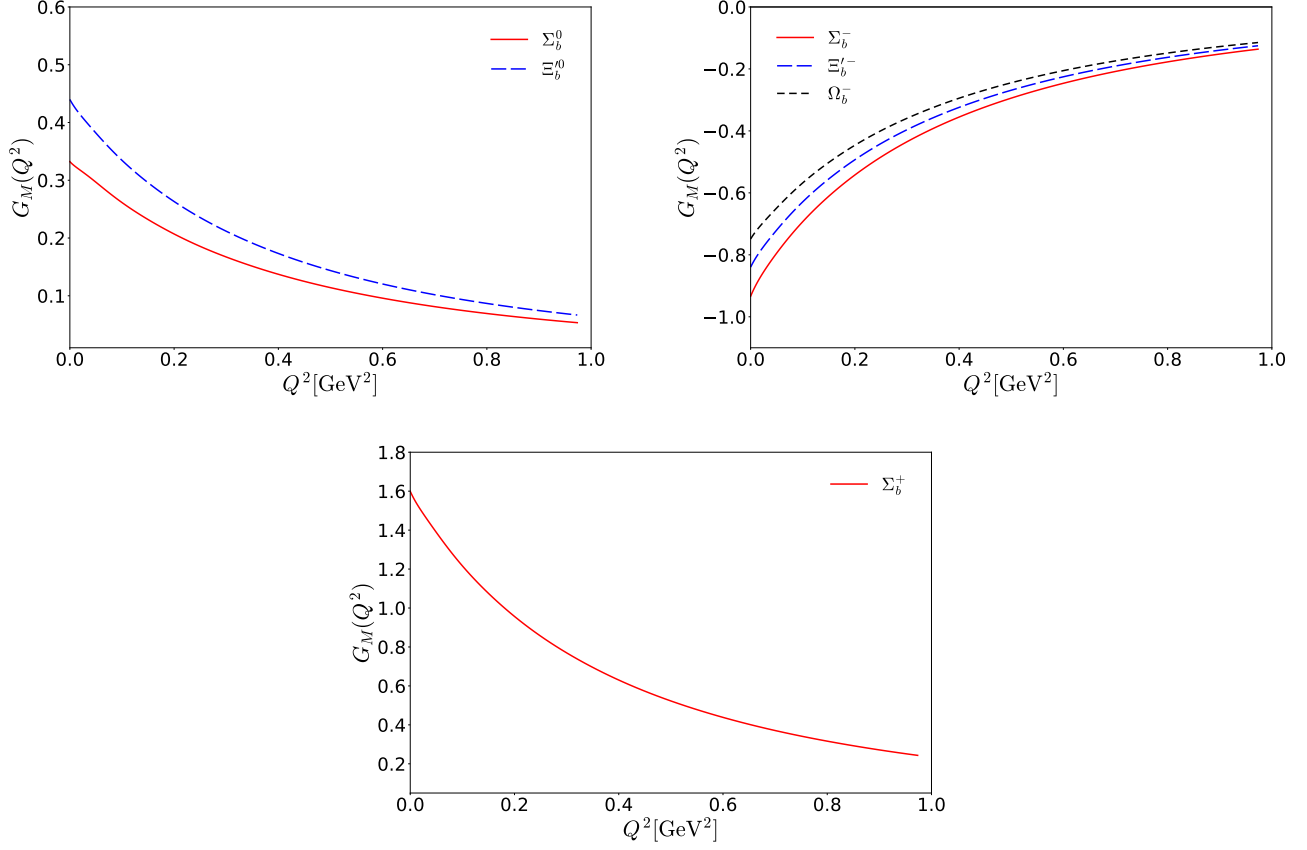


FIG. 13. Magnetic form factors of the bottom baryon sextet with  $J' = 1/2$ .

corresponding baryons [10], Eq. (37) is identical to the sum of  $2Q - 1$  for all the members of the baryon sextet, where  $Q$  denotes the charge of the corresponding heavy baryon in the sextet. Thus, Eq. (37) is satisfied. Note that Eq. (37) is no more valid when the effects of  $SU_f(3)$  symmetry breaking are considered.

TABLE III. Magnetic moments of the charmed baryon sextet with spin 1/2 in comparison with various models. The results are given in units of the nuclear magneton  $\mu_N$ .

Baryon	$\mu_{B_c}^{(m_s=0 \text{ MeV})}$	$\mu_{B_c}^{(m_s=174 \text{ MeV})}$	[35]	[46]	[47]	[48]	[49]	[33, 52]
$\Sigma_c^{++}$	1.58	1.60	$2.15 \pm 0.1$	1.95	2.45	1.76	$1.50^{+0.18}_{-0.20}$	$2.220 \pm 0.505$
$\Sigma_c^+$	0.39	0.33	$0.46 \pm 0.03$	0.41	0.25	0.36	$0.12^{0.06}_{-0.10}$	–
$\Sigma_c^0$	-0.79	-0.94	$-1.24 \pm 0.05$	-1.1	-1.96	-1.04	$-1.25^{+0.08}_{-0.08}$	$-1.073 \pm 0.269$
$\Xi_c^+$	0.39	0.44	$0.60 \pm 0.02$	0.77	–	0.47	$0.32^{+0.13}_{-0.11}$	$0.315 \pm 0.141$
$\Xi_c^0$	-0.79	-0.84	$-1.05 \pm 0.04$	-1.12	–	-0.95	$-0.95^{+0.08}_{-0.05}$	$-0.599 \pm 0.071$
$\Omega_c^0$	-0.79	-0.75	$-0.85 \pm 0.05$	-0.79	–	-0.85	$-0.67^{+0.09}_{-0.09}$	$-0.639 \pm 0.088$

While there are very few theoretical works on the EM form factors of the heavy baryons [50, 51], the magnetic moments of the heavy baryons have been studied within various theoretical models. In this work, we compare the present results of the magnetic moments with those of Refs. [33, 35, 46–49, 52]. In Table III, we list the results of the magnetic moments of the baryon sextet with spin 1/2. In the second and third columns, the results of the magnetic moments without and with the linear  $m_s$  corrections, respectively. The effects of the  $SU_f(3)$  symmetry breaking are in the range of 2% – 20%. For example, the  $\Omega_c^0$  magnetic moment acquires a marginal contribution from the  $m_s$  corrections, whereas  $\Sigma_c^0$  gets about 20% corrections. We first compare the results with those from Ref. [35] where the same framework was used but the dynamical parameters  $w_i$  were fixed by using the experimental data on those of the baryon octet. We see that the magnitudes of the results are consistently smaller than those of Ref. [35]. Except for the  $\Omega_c^0$  magnetic moment, the present results are in general smaller than those of Ref. [46] where the Skyrme

TABLE IV. Magnetic moments of the bottom baryon sextet with spin 1/2 in units of the nuclear magneton  $\mu_N$ .

	$\mu_{B_b}^{(m_s=0 \text{ MeV})}$	$\mu_{B_b}^{(m_s=166 \text{ MeV})}$	[35]	[47]	[48]
$\Sigma_b^+$	1.58	1.60	$2.15 \pm 0.1$	2.52	2.07
$\Sigma_b^0$	0.39	0.33	$0.46 \pm 0.03$	0.29	0.53
$\Sigma_b^-$	-0.79	-0.93	$-1.24 \pm 0.05$	-1.94	-1.01
$\Xi_b^{\prime 0}$	0.39	0.44	$0.60 \pm 0.02$	-	0.66
$\Xi_b^{\prime -}$	-0.79	-0.84	$-1.05 \pm 0.04$	-	-0.91
$\Omega_b^-$	-0.79	-0.75	$-0.85 \pm 0.05$	-	-0.82

model with the bound-state approach was employed. Reference [47] extended the model used in Ref. [46], including the vector mesons. The results of the  $\Sigma_c^{++}$  and  $\Sigma_c^0$  turn out to be the largest in size among all other models. On the other hand, that of  $\Sigma_c^+$  from Ref. [47] is the smallest. Interestingly, the results of Ref. [48] are very similar to the present ones, even though the relativistic three-quark model of Ref. [48] is very different from the present approach. In the final column, the lattice results are given [33, 52], which show qualitatively a similar tendency. In Table IV, we list the results of the bottom baryon sextet with spin 1/2 for completeness. The results are basically the same as those of the charmed baryons.

TABLE V. Magnetic radii of the charmed baryon sextet with spin 1/2 in units of  $\text{fm}^2$ .

Baryon	$\langle r^2 \rangle_M^{B_c(m_s=0 \text{ MeV})}$	$\langle r^2 \rangle_M^{B_c(m_s=174 \text{ MeV})}$	[33]
$\Sigma_c^{++}$	0.62	0.62	$0.696 \pm 0.153$
$\Sigma_c^+$	0.62	0.40	-
$\Sigma_c^0$	0.62	0.78	$0.650 \pm 0.126$
$\Xi_c^+$	0.62	0.63	-
$\Xi_c^0$	0.62	0.72	-
$\Omega_c^0$	0.62	0.64	$0.354 \pm 0.054$

The magnetic radius is defined by

$$\langle r^2 \rangle_M^{B_Q} = -\frac{6}{\mu_B} \left. \frac{dG_M^B(Q^2)}{dQ^2} \right|_{Q^2=0}. \quad (38)$$

In Table V, the numerical results of Eq. (38) are listed in comparison with the lattice data. When the linear  $m_s$  corrections are switched off, all the results turn out to be the same. This can be easily understood. As shown in Eq. (38) the magnetic radius is normalized by the magnetic moment of the corresponding heavy baryon. In the present mean-field formalism, we find that the flavor part or the  $D$ -function part of the derivative of the magnetic form factor is canceled by the normalization due to the magnetic moment. Thus, all the magnetic radii of the lowest-lying baryon sextet with spin 1/2 are expressed by the single equation

$$\langle r^2 \rangle_M^{\Sigma_c^{++}} = \langle r^2 \rangle_M^{\Sigma_c^+} = \langle r^2 \rangle_M^{\Sigma_c^0} = \langle r^2 \rangle_M^{\Xi_c^+} = \langle r^2 \rangle_M^{\Xi_c^0} = \langle r^2 \rangle_M^{\Omega_c^0}. \quad (39)$$

This is the unique feature of the model and moreover Eq. (39) is a special case of the  $U$ -spin relation. Note that the magnetic radii of the baryon octet do not satisfy this relation. The present results of the magnetic radii are compared with those from the lattice calculation [33]. Except for the  $\Omega_c^0$ , we find that the results are in qualitative agreement with the lattice data. Table VI lists the results of the magnetic radii for the bottom baryon sextet with spin 1/2. As mentioned several times already, The results have no difference from those for the charmed baryons because of the present mean-field approach.

TABLE VI. Magnetic radii of the bottom baryon sextet with spin 1/2 in units of  $\text{fm}^2$ .

Baryon	$\langle r^2 \rangle_M^{B_b(m_s=0 \text{ MeV})}$	$\langle r^2 \rangle_M^{B_b(m_s=166 \text{ MeV})}$
$\Sigma_b^+$	0.62	0.62
$\Sigma_b^0$	0.62	0.42
$\Sigma_b^-$	0.62	0.77
$\Xi_b^0$	0.62	0.63
$\Xi_b^-$	0.62	0.71
$\Omega_b^-$	0.62	0.64



#### IV. SUMMARY AND CONCLUSION

In the present work, we have investigated the electromagnetic properties of the lowest-lying singly heavy baryons with spin  $1/2$  within the framework of the chiral quark-soliton model. The model is a pion mean-field approach in which a baryon is viewed as  $N_c$  valence quarks bound by the pion mean fields created self-consistently. In the same manner, a singly heavy baryon can be regarded as  $N_c - 1$  valence quarks in the presence of the pion mean fields, its mass being assumed to be infinitely heavy. In this limit of the infinite heavy-quark mass, the heavy quark inside a singly heavy baryon can be treated as a mere static color source. Thus, the structure of the heavy baryon is mainly governed by the light-quark dynamics. In the chiral quark-soliton model, the constraint on the quantization rule is imposed by the number of valence quarks. In the case of light baryons, the right hypercharge is constrained to be  $Y' = N_c/3$ . Since the singly heavy quark, however, consists of the  $N_c - 1$  valence quarks with the heavy quark stripped off, the quantization rule should be modified by  $Y' = (N_c - 1)/3$ . Then the quantization naturally yields the baryon antitriplet and the baryon sextet with both spins  $1/2$  and  $3/2$ .

We first studied the electric properties of the baryon antitriplet and sextet with spin  $1/2$ . The results show that the  $Q^2$  dependence of the electric form factors for the positive-charged heavy baryons is very similar. Comparison of these results with that of the proton electric form factor points to the conclusion that the heavy baryon is an electrically compact object. The result of the  $\Sigma_c^{++}$  electric form factor was compared with the lattice data. As anticipated, the present result falls off faster than the lattice one as  $Q^2$  increases. Keeping in mind that all the lattice results of the proton electric form factor overestimate the experimental data when the unphysical pion mass is employed, we are able to state that the present mean-field approach produce the consistent results of the electric form factors of the positive-charged heavy baryons. We also computed the electric form factors of the neutral heavy baryons. The results of the electric charge radii were also presented. We found that the effects of  $SU_f(3)$  symmetry breaking are marginal.

Since the heavy baryons in the antitriplet contain the light-quark pair in spin zero in the present scheme, the magnetic form factors vanish. So, we concentrated on those of the baryon sextet with spin  $1/2$ . The magnetic densities of the positive-charge heavy baryons are very similar to that of the proton, whereas the neutral ones take after the neutron one. The results show that the magnetic form factors of the heavy baryons fall off monotonically as  $Q^2$  increases. The results of the magnetic moments were compared with those from various works and were found to be consistent each other, though there are differences quantitatively. The magnetic radii were also calculated. Interestingly, when the effects of flavor  $SU(3)$  symmetry breaking are turned off, all the magnetic radii of the heavy baryons turn out to be the same. This arises from the fact that the flavor parts of the magnetic form factors are exactly canceled by the normalizations, i.e., magnetic moments. This can be also understood as a special case of the  $U$ -spin relation.

In conclusion, the present pion mean-field approach describes the electromagnetic properties of the lowest-lying singly heavy baryons consistently, compared with other models and lattice QCD. Thus, a singly heavy baryon is indeed mainly explained by the light quarks inside it, while the heavy quark remains as a static color source. Of course the effects of higher-order corrections in the expansion of the heavy quark mass should be required in order to describe the electromagnetic properties of the heavy baryons. This is a very interesting issue for the future works. It is also of great interest to study the electromagnetic form factors of the sextet baryon with spin  $3/2$ . As in the case of the baryon decuplet, we have additionally more form factors for the spin- $3/2$  heavy baryons such as the electric quadrupole and magnetic octupole form factors. The corresponding work is under way.

#### ACKNOWLEDGMENTS

The authors are grateful to Gh.-S. Yang for valuable discussion. They also want to express their gratitude to K. U. Can and M. Oka for providing them with the lattice data on the electromagnetic form factors of the heavy baryons. The present work was supported by Basic Science Research Program through the National Research Foundation of Korea funded by the Ministry of Education, Science and Technology (Grant No. NRF-2018R1A2B2001752).

#### Appendix A: Matrix elements of the $SU(3)$ Wigner $D$ function

In the following, we list in Tables VII-XIV the results of the matrix elements of the relevant collective operators for the EM form factors of the heavy baryons.

TABLE VII. The matrix elements of the collective operators of the leading terms and the  $1/N_c$  rotational corrections to the electric form factors.

$$\begin{aligned}
& \langle \Lambda_c | D_{88}^{(8)} | \Lambda_c \rangle = \langle \Xi_c | D_{88}^{(8)} | \Xi_c \rangle = \frac{3}{8} Y \\
& \langle \Lambda_c | D_{38}^{(8)} | \Lambda_c \rangle = \langle \Xi_c | D_{38}^{(8)} | \Xi_c \rangle = \frac{\sqrt{3}}{4} T_3 \\
& \langle \Lambda_c | D_{8i}^{(8)} J_i | \Lambda_c \rangle = \langle \Xi_c | D_{8i}^{(8)} J_i | \Xi_c \rangle = \langle \Lambda_c | D_{3i}^{(8)} J_i | \Lambda_c \rangle = \langle \Xi_c | D_{3i}^{(8)} J_i | \Xi_c \rangle = 0 \\
& \langle \Lambda_c | D_{8a}^{(8)} J_a | \Lambda_c \rangle = \langle \Xi_c | D_{8a}^{(8)} J_a | \Xi_c \rangle = -\frac{3\sqrt{3}}{8} Y \\
& \langle \Lambda_c | D_{3a}^{(8)} J_a | \Lambda_c \rangle = \langle \Xi_c | D_{3a}^{(8)} J_a | \Xi_c \rangle = -\frac{3}{4} T_3 \\
\hline
& \langle \Sigma_c | D_{88}^{(8)} | \Sigma_c \rangle = \langle \Xi'_c | D_{88}^{(8)} | \Xi'_c \rangle = \langle \Omega_c | D_{88}^{(8)} | \Omega_c \rangle = \frac{3}{20} Y \\
& \langle \Sigma_c | D_{38}^{(8)} | \Sigma_c \rangle = \langle \Xi'_c | D_{38}^{(8)} | \Xi'_c \rangle = \langle \Omega_c | D_{38}^{(8)} | \Omega_c \rangle = \frac{\sqrt{3}}{10} T_3 \\
& \langle \Sigma_c | D_{8i}^{(8)} J_i | \Sigma_c \rangle = \langle \Xi'_c | D_{8i}^{(8)} J_i | \Xi'_c \rangle = \langle \Omega_c | D_{8i}^{(8)} J_i | \Omega_c \rangle = -\frac{3\sqrt{3}}{10} Y \\
& \langle \Sigma_c | D_{3i}^{(8)} J_i | \Sigma_c \rangle = \langle \Xi'_c | D_{3i}^{(8)} J_i | \Xi'_c \rangle = \langle \Omega_c | D_{3i}^{(8)} J_i | \Omega_c \rangle = -\frac{3}{5} T_3 \\
& \langle \Sigma_c | D_{8a}^{(8)} J_a | \Sigma_c \rangle = \langle \Xi'_c | D_{8a}^{(8)} J_a | \Xi'_c \rangle = \langle \Omega_c | D_{8a}^{(8)} J_a | \Omega_c \rangle = -\frac{3\sqrt{3}}{20} Y \\
& \langle \Sigma_c | D_{3a}^{(8)} J_a | \Sigma_c \rangle = \langle \Xi'_c | D_{3a}^{(8)} J_a | \Xi'_c \rangle = \langle \Omega_c | D_{3a}^{(8)} J_a | \Omega_c \rangle = -\frac{3}{10} T_3
\end{aligned}$$

TABLE VIII. The matrix elements of the collective operators of the leading terms and the  $1/N_c$  rotational corrections to the magnetic form factors.

$$\begin{aligned}
& \langle \Sigma_c | D_{33}^{(8)} | \Sigma_c \rangle = \langle \Xi'_c | D_{33}^{(8)} | \Xi'_c \rangle = \langle \Omega_c | D_{33}^{(8)} | \Omega_c \rangle = -\frac{1}{5} T_3 \\
& \langle \Sigma_c | D_{83}^{(8)} | \Sigma_c \rangle = \langle \Xi'_c | D_{83}^{(8)} | \Xi'_c \rangle = \langle \Omega_c | D_{83}^{(8)} | \Omega_c \rangle = -\frac{3}{10\sqrt{3}} Y \\
& \langle \Sigma_c | D_{38}^{(8)} J_3 | \Sigma_c \rangle = \langle \Xi'_c | D_{38}^{(8)} J_3 | \Xi'_c \rangle = \langle \Omega_c | D_{38}^{(8)} J_3 | \Omega_c \rangle = \frac{1}{5\sqrt{3}} T_3 \\
& \langle \Sigma_c | D_{88}^{(8)} J_3 | \Sigma_c \rangle = \langle \Xi'_c | D_{88}^{(8)} J_3 | \Xi'_c \rangle = \langle \Omega_c | D_{88}^{(8)} J_3 | \Omega_c \rangle = \frac{1}{10} Y \\
& \langle \Sigma_c | d_{ab3} D_{3a}^{(8)} J_b | \Sigma_c \rangle = \langle \Xi'_c | d_{ab3} D_{3a}^{(8)} J_b | \Xi'_c \rangle = \langle \Omega_c | d_{ab3} D_{3a}^{(8)} J_b | \Omega_c \rangle = \frac{1}{10} T_3 \\
& \langle \Sigma_c | d_{ab3} D_{8a}^{(8)} J_b | \Sigma_c \rangle = \langle \Xi'_c | d_{ab3} D_{8a}^{(8)} J_b | \Xi'_c \rangle = \langle \Omega_c | d_{ab3} D_{8a}^{(8)} J_b | \Omega_c \rangle = \frac{3}{20\sqrt{3}} Y
\end{aligned}$$

### Appendix B: Dynamical coefficients $w_i$ for the magnetic moments

In Eq. (29), the collective operator for the magnetic moments are defined in terms of the dynamical coefficients  $w_i$  that are expressed as

$$\begin{aligned}
w_1 &= \int d^3 z \frac{M_N}{3} \left( Q_0(\mathbf{z}) + \frac{1}{I_1} Q_1(\mathbf{z}) - 2M_1 \mathcal{M}_0(\mathbf{z}) \right) \\
w_2 &= -\frac{1}{I_2} \int d^3 z \frac{M_N}{3} \mathcal{X}_2(\mathbf{z}) \\
w_3 &= -\frac{1}{I_1} \int d^3 z \frac{M_N}{3} \mathcal{X}_1(\mathbf{z}) \\
w_4 &= 2\sqrt{3} M_8 \int d^3 z \frac{M_N}{3} \left( \frac{K_2}{I_2} \mathcal{X}_2(\mathbf{z}) - \mathcal{M}_2(\mathbf{z}) \right) \\
w_5 &= \frac{1}{\sqrt{3}} M_8 \int d^3 z \frac{M_N}{3} \left( \frac{K_1}{I_1} \mathcal{X}_1(\mathbf{z}) - \mathcal{M}_1(\mathbf{z}) - \mathcal{M}_0(\mathbf{z}) \right) \\
w_6 &= -\frac{1}{\sqrt{3}} M_8 \int d^3 z \frac{M_N}{3} \left( \frac{K_1}{I_1} \mathcal{X}_1(\mathbf{z}) - \mathcal{M}_1(\mathbf{z}) + \mathcal{M}_0(\mathbf{z}) \right). \tag{B1}
\end{aligned}$$

The results of  $w_i$  are listed in Table XV in comparison with those from Ref. [35], where  $w_i$  were determined by using the experimental data on the magnetic moments of the baryon octet.

- 
- [1] E. Witten, Nucl. Phys. **B160**, 57 (1979).  
[2] E. Witten, Nucl. Phys. **B223**, 433 (1983).

TABLE IX. The matrix elements of the collective operators of the  $m_s$  corrections to the electric form factors.

$\mathcal{R}$ B	$\mathbf{3}$		$\mathbf{6}$		
	$\Lambda_c$	$\Xi_c$	$\Sigma_c$	$\Xi'_c$	$\Omega_c$
$\langle B_{\mathcal{R}}   D_{8i}^{(8)} D_{3i}^{(8)}   B_{\mathcal{R}} \rangle$	0	$\frac{3\sqrt{3}}{20} T_3$	$\frac{11}{60\sqrt{3}} T_3$	$\frac{1}{6\sqrt{3}} T_3$	0
$\langle B_{\mathcal{R}}   D_{8i}^{(8)} D_{8i}^{(8)}   B_{\mathcal{R}} \rangle$	$\frac{9}{40}$	$\frac{9}{20}$	$\frac{19}{60}$	$\frac{2}{5}$	$\frac{1}{2}$
$\langle B_{\mathcal{R}}   D_{8a}^{(8)} D_{3a}^{(8)}   B_{\mathcal{R}} \rangle$	0	$-\frac{\sqrt{3}}{10} T_3$	$-\frac{2}{15\sqrt{3}} T_3$	$-\frac{1}{15\sqrt{3}} T_3$	0
$\langle B_{\mathcal{R}}   D_{8a}^{(8)} D_{8a}^{(8)}   B_{\mathcal{R}} \rangle$	$\frac{3}{5}$	$\frac{9}{20}$	$\frac{8}{15}$	$\frac{1}{2}$	$\frac{2}{5}$
$\langle B_{\mathcal{R}}   D_{88}^{(8)} D_{38}^{(8)}   B_{\mathcal{R}} \rangle$	0	$-\frac{\sqrt{3}}{20} T_3$	$-\frac{1}{20\sqrt{3}} T_3$	$-\frac{1}{40\sqrt{3}} T_3$	0
$\langle B_{\mathcal{R}}   D_{88}^{(8)} D_{88}^{(8)}   B_{\mathcal{R}} \rangle$	$\frac{7}{40}$	$\frac{1}{10}$	$\frac{3}{20}$	$\frac{1}{10}$	$\frac{1}{10}$

TABLE X. The matrix elements of the collective operators of the  $m_s$  corrections to the magnetic form factors.

$\mathcal{R}$ B	$\mathbf{6}$		
	$\Sigma_c$	$\Xi'_c$	$\Omega_c$
$\langle B_{\mathcal{R}}   D_{88}^{(8)} D_{33}^{(8)}   B_{\mathcal{R}} \rangle$	$-\frac{2}{45} T_3$	$-\frac{1}{45} T_3$	0
$\langle B_{\mathcal{R}}   D_{88}^{(8)} D_{83}^{(8)}   B_{\mathcal{R}} \rangle$	$\frac{1}{30\sqrt{3}}$	0	$-\frac{1}{10\sqrt{3}}$
$\langle B_{\mathcal{R}}   D_{83}^{(8)} D_{38}^{(8)}   B_{\mathcal{R}} \rangle$	$-\frac{2}{45} T_3$	$-\frac{1}{45} T_3$	0
$\langle B_{\mathcal{R}}   D_{83}^{(8)} D_{88}^{(8)}   B_{\mathcal{R}} \rangle$	$\frac{1}{30\sqrt{3}}$	0	$-\frac{1}{10\sqrt{3}}$
$\langle B_{\mathcal{R}}   d_{ab3} D_{8a}^{(8)} D_{8b}^{(8)}   B_{\mathcal{R}} \rangle$	$\frac{2}{45}$	$-\frac{1}{30}$	$-\frac{1}{15}$
$\langle B_{\mathcal{R}}   d_{ab3} D_{3a}^{(8)} D_{8b}^{(8)}   B_{\mathcal{R}} \rangle$	$-\frac{1}{9\sqrt{3}} T_3$	$-\frac{7}{45\sqrt{3}} T_3$	0

- [3] D. Diakonov, V. Y. Petrov, and P. V. Pobylitsa, Nucl. Phys. **B306**, 809 (1988).  
[4] M. Wakamatsu and H. Yoshiki, Nucl. Phys. **A524**, 561 (1991).  
[5] C. V. Christov, A. Blotz, H.-Ch. Kim, P. Pobylitsa, T. Watabe, T. Meissner, E. Ruiz Arriola, and K. Goeke, Prog. Part. Nucl. Phys. **37**, 91 (1996).  
[6] D. Diakonov, arXiv:hep-ph/9802298.  
[7] H.-Ch. Kim, A. Blotz, M. V. Polyakov, and K. Goeke, Phys. Rev. D **53**, 4013 (1996).  
[8] H.-Ch. Kim, M. V. Polyakov, A. Blotz, and K. Goeke, Nucl. Phys. **A598**, 379 (1996).  
[9] M. Wakamatsu and N. Kaya, Prog. Theor. Phys. **95**, 767 (1996).  
[10] H.-Ch. Kim, M. Praszalowicz, and K. Goeke, Phys. Rev. D **57**, 2859 (1998).  
[11] A. Silva, D. Urbano, and H.-Ch. Kim, Prog. Theor. Exp. Phys. **2018**, 023D01 (2018).  
[12] A. Silva, H.-Ch. Kim, D. Urbano, and K. Goeke, Phys. Rev. D **72**, 094011 (2005).  
[13] H.-Ch. Kim, M. V. Polyakov, and K. Goeke, Phys. Rev. D **53**, R4715 (1996).  
[14] H.-Ch. Kim, M. V. Polyakov, and K. Goeke, Phys. Lett. B **387**, 577 (1996).  
[15] P. V. Pobylitsa and M. V. Polyakov, Phys. Lett. B **389**, 350 (1996).  
[16] P. Schweitzer, D. Urbano, M. V. Polyakov, C. Weiss, P. V. Pobylitsa, and K. Goeke, Phys. Rev. D **64**, 034013 (2001).  
[17] T. Ledwig, A. Silva, and H.-Ch. Kim, Phys. Rev. D **82**, 034022 (2010).  
[18] T. Ledwig, A. Silva, and H.-Ch. Kim, Phys. Rev. D **82**, 054014 (2010).  
[19] H.-Ch. Kim, M. V. Polyakov, M. Praszalowicz, and K. Goeke, Phys. Rev. D **57**, 299 (1998).  
[20] T. Ledwig, A. Silva, H.-Ch. Kim, and K. Goeke, J. High Energy Phys. 07 (2008) 132.  
[21] G. S. Yang and H.-Ch. Kim, Phys. Rev. C **92**, 035206 (2015).  
[22] D. Diakonov, V. Petrov, P. Pobylitsa, M. V. Polyakov, and C. Weiss, Nucl. Phys. **B480**, 341 (1996).  
[23] D. Diakonov, V. Y. Petrov, P. V. Pobylitsa, M. V. Polyakov, and C. Weiss, Phys. Rev. D **56**, 4069 (1997).  
[24] M. Wakamatsu and T. Kubota, Phys. Rev. D **57**, 5755 (1998).  
[25] Gh.-S. Yang, H.-Ch. Kim, M. V. Polyakov, and M. Praszalowicz, Phys. Rev. D **94**, 071502 (2016).  
[26] D. Diakonov, arXiv:1003.2157.  
[27] N. Isgur and M. B. Wise, Phys. Lett. B **232**, 113 (1989).  
[28] H. Georgi, Phys. Lett. B **240**, 447 (1990).  
[29] J. Y. Kim, H.-Ch. Kim, and G. S. Yang, arXiv:1801.09405.  
[30] H.-Ch. Kim, M. V. Polyakov, and M. Praszalowicz, Phys. Rev. D **96**, 014009 (2017); **96**, 039902(E) (2017).  
[31] R. Aaij *et al.* (LHCb Collaboration), Phys. Rev. Lett. **118**, 182001 (2017).  
[32] H.-Ch. Kim, M. V. Polyakov, M. Praszalowicz, and G. S. Yang, Phys. Rev. D **96**, 094021 (2017).  
[33] K. U. Can, G. Erkol, B. Isildak, M. Oka, and T. T. Takahashi, J. High Energy Phys. 05, (2014) 125.  
[34] T. Ledwig, H. C. Kim, and K. Goeke, Nucl. Phys. **A811**, 353 (2008).

TABLE XI. The relevant transition matrix elements of the collective operators coming from the anti-15plet component of the baryon wave functions for the electric form factors.

$\mathcal{R}$ $B$	$\mathbf{3}$		$\mathbf{6}$		
	$\Lambda_c$	$\Xi_c$	$\Sigma_c$	$\Xi'_c$	$\Omega_c$
$\langle B_{\overline{15}}   D_{88}^{(8)}   B_{\mathcal{R}} \rangle$	$\frac{3}{4\sqrt{5}}$	$\frac{3}{8}\sqrt{\frac{3}{5}}$	$\sqrt{\frac{1}{10}}$	$\frac{1}{4}\sqrt{\frac{3}{5}}$	0
$\langle B_{\overline{15}}   D_{38}^{(8)}   B_{\mathcal{R}} \rangle$	0	$-\frac{1}{4\sqrt{5}}T_3$	$-\frac{1}{\sqrt{30}}T_3$	$-\frac{\sqrt{5}}{6}T_3$	0
$\langle B_{\overline{15}}   D_{8i}^{(8)} J_i   B_{\mathcal{R}} \rangle$	0	0	$\sqrt{\frac{2}{15}}$	$\frac{1}{2\sqrt{5}}$	0
$\langle B_{\overline{15}}   D_{3i}^{(8)} J_i   B_{\mathcal{R}} \rangle$	0	0	$-\frac{1}{3}\sqrt{\frac{2}{5}}T_3$	$-\frac{1}{3}\sqrt{\frac{5}{3}}T_3$	0
$\langle B_{\overline{15}}   D_{8a}^{(8)} J_a   B_{\mathcal{R}} \rangle$	$\frac{1}{4}\sqrt{\frac{3}{5}}$	$\frac{3}{8}\sqrt{\frac{1}{5}}$	$-\sqrt{\frac{1}{30}}$	$-\frac{1}{4\sqrt{5}}$	0
$\langle B_{\overline{15}}   D_{3a}^{(8)} J_a   B_{\mathcal{R}} \rangle$	0	$-\frac{1}{4}\sqrt{\frac{1}{15}}T_3$	$\frac{1}{3}\sqrt{\frac{1}{10}}T_3$	$\frac{1}{6}\sqrt{\frac{5}{3}}T_3$	0

TABLE XII. The relevant transition matrix elements of the collective operators coming from the anti-24plet component of the baryon wave functions for the electric form factors.

$\mathcal{R}$ $B$	$\mathbf{3}$		$\Sigma_c$	$\Xi'_c$	$\Omega_c$
	$\Lambda_c$	$\Xi_c$			
$\langle B_{\overline{24}}   D_{88}^{(8)}   B_{\mathcal{R}} \rangle$	0	0	$\frac{1}{5}$	$\frac{1}{5}\sqrt{\frac{3}{2}}$	$\frac{1}{5}\sqrt{\frac{3}{2}}$
$\langle B_{\overline{24}}   D_{38}^{(8)}   B_{\mathcal{R}} \rangle$	0	0	$\frac{1}{10\sqrt{3}}T_3$	$\frac{2}{15\sqrt{2}}T_3$	0
$\langle B_{\overline{24}}   D_{8i}^{(8)} J_i   B_{\mathcal{R}} \rangle$	0	0	$-\frac{1}{5\sqrt{3}}$	$-\frac{1}{5\sqrt{2}}$	$-\frac{1}{5\sqrt{2}}$
$\langle B_{\overline{24}}   D_{3i}^{(8)} J_i   B_{\mathcal{R}} \rangle$	0	0	$-\frac{1}{30}T_3$	$-\frac{2}{15}\sqrt{\frac{1}{6}}T_3$	0
$\langle B_{\overline{24}}   D_{8a}^{(8)} J_a   B_{\mathcal{R}} \rangle$	0	0	$\frac{2}{5}\sqrt{\frac{1}{3}}$	$\frac{\sqrt{2}}{5}$	$\frac{\sqrt{2}}{5}$
$\langle B_{\overline{24}}   D_{3a}^{(8)} J_a   B_{\mathcal{R}} \rangle$	0	0	$\frac{1}{15}T_3$	$\frac{2}{15}\sqrt{\frac{2}{3}}T_3$	0

- [35] G. S. Yang and H.-Ch. Kim, Phys. Lett. B **781**, 601 (2018).  
[36] M. Praszalowicz, T. Watabe, and K. Goeke, Nucl. Phys. **A647**, 49 (1999).  
[37] V. Sulkosky *et al.*, Phys. Rev. C **96**, 065206 (2017).  
[38] S. Capitani *et al.*, Phys. Rev. D **92**, 054511 (2015).  
[39] A. Abdel-Rehim, C. Alexandrou, M. Constantinou, K. Hadjiyiannakou, K. Jansen, and G. Koutsou, Proc. Sci., LATTICE2014 (**2015**) 148 [arXiv:1501.01480].  
[40] D. Djukanovic, T. Harris, G. von Hippel, P. Junnarkar, H. B. Meyer, and H. Wittig, Proc. Sci., LATTICE2015 **2016**, 137. [arXiv:1511.07481].  
[41] A. J. Chambers *et al.* (QCDSF and UKQCD and CSSM Collaborations), Phys. Rev. D **96**, 114509 (2017).  
[42] C. Alexandrou, M. Constantinou, K. Hadjiyiannakou, K. Jansen, C. Kallidonis, G. Koutsou, and A. Vaquero Aviles-Casco, Phys. Rev. D **96**, 034503 (2017).  
[43] M. Gockeler *et al.* (QCDSF and UKQCD Collaborations), Phys. Lett. B **627**, 113 (2005).  
[44] M. Gockeler *et al.* (QCDSF and UKQCD Collaborations), Phys. Rev. Lett. **98**, 222001 (2007).  
[45] C. Patrignani *et al.* (Particle Data Group), Chin. Phys. C, **40**, 100001 (2016) and 2017 update.  
[46] Y. s. Oh, D. P. Min, M. Rho, and N. N. Scoccola, Nucl. Phys. **A534**, 493 (1991).  
[47] S. Scholl and H. Weigel, Nucl. Phys. **A735**, 163 (2004).  
[48] A. Faessler, T. Gutsche, M. A. Ivanov, J. G. Korner, V. E. Lyubovitskij, D. Nicmorus, and K. Pumsa-ard, Phys. Rev. D **73**, 094013 (2006).  
[49] G. J. Wang, L. Meng, H. S. Li, Z. W. Liu, and S. L. Zhu, arXiv:1803.00229.  
[50] L. L. Liu, C. Wang, and X. H. Guo, arXiv:1801.08417.  
[51] L. L. Liu, C. Wang, Y. Liu, and X. H. Guo, Phys. Rev. D **95**, 054001 (2017).  
[52] H. Bahtiyar, K. U. Can, G. Erkol, M. Oka, and T. T. Takahashi, Phys. Lett. B **772**, 121 (2017).

TABLE XIII. The relevant transition matrix elements of the collective operators coming from the anti-15plet component of the baryon wave functions for the magnetic form factors.

$\mathcal{R}$ B	$\mathbf{6}$		
	$\Sigma_c$	$\Xi'_c$	$\Omega_c$
$\langle B_{\overline{15}}   D_{33}^{(8)}   B_{\mathcal{R}} \rangle$	$-\frac{1}{9} \sqrt{\frac{2}{5}} T_3$	$-\frac{1}{9} \sqrt{\frac{5}{3}} T_3$	0
$\langle B_{\overline{15}}   D_{83}^{(8)}   B_{\mathcal{R}} \rangle$	$\frac{1}{3} \sqrt{\frac{2}{15}}$	$\frac{1}{6\sqrt{5}}$	0
$\langle B_{\overline{15}}   D_{38}^{(8)} J_3   B_{\mathcal{R}} \rangle$	$-\frac{1}{3} \sqrt{\frac{2}{15}} T_3$	$-\frac{\sqrt{5}}{9} T_3$	0
$\langle B_{\overline{15}}   D_{88}^{(8)} J_3   B_{\mathcal{R}} \rangle$	$\frac{1}{3} \sqrt{\frac{2}{5}}$	$\frac{1}{2\sqrt{15}}$	0
$\langle B_{\overline{15}}   d_{ab3} D_{3a}^{(8)} J_b   B_{\mathcal{R}} \rangle$	$-\frac{1}{9\sqrt{10}} T_3$	$-\frac{1}{18} \sqrt{\frac{5}{3}} T_3$	0
$\langle B_{\overline{15}}   d_{ab3} D_{8a}^{(8)} J_b   B_{\mathcal{R}} \rangle$	$\frac{1}{3\sqrt{30}}$	$\frac{1}{12\sqrt{5}}$	0

TABLE XIV. The relevant transition matrix elements of the collective operators coming from the anti-24plet component of the baryon wave functions for the magnetic form factors.

$\mathcal{R}$ B	$\mathbf{6}$		
	$\Sigma_c$	$\Xi'_c$	$\Omega_c$
$\langle B_{\overline{24}}   D_{33}^{(8)}   B_{\mathcal{R}} \rangle$	$-\frac{1}{90} T_3$	$-\frac{2}{45\sqrt{6}} T_3$	0
$\langle B_{\overline{24}}   D_{83}^{(8)}   B_{\mathcal{R}} \rangle$	$-\frac{1}{15\sqrt{3}}$	$-\frac{1}{15\sqrt{2}}$	$-\frac{1}{15\sqrt{2}}$
$\langle B_{\overline{24}}   D_{38}^{(8)} J_3   B_{\mathcal{R}} \rangle$	$\frac{1}{15\sqrt{3}} T_3$	$\frac{2\sqrt{2}}{45} T_3$	0
$\langle B_{\overline{24}}   D_{88}^{(8)} J_3   B_{\mathcal{R}} \rangle$	$\frac{2}{15}$	$\frac{1}{5} \sqrt{\frac{2}{3}}$	$\frac{1}{5} \sqrt{\frac{2}{3}}$
$\langle B_{\overline{24}}   d_{ab3} D_{3a}^{(8)} J_b   B_{\mathcal{R}} \rangle$	$-\frac{1}{45} T_3$	$-\frac{2}{45} \sqrt{\frac{2}{3}} T_3$	0
$\langle B_{\overline{24}}   d_{ab3} D_{8a}^{(8)} J_b   B_{\mathcal{R}} \rangle$	$-\frac{2}{15\sqrt{3}}$	$-\frac{\sqrt{2}}{15}$	$-\frac{\sqrt{2}}{15}$

TABLE XV. Magnetic  $\chi$  QSM parameters for  $M = 420\text{MeV}$  heavy baryon.

	$w_1$	$w_2$	$w_3$	$w_4$	$w_5$	$w_6$
Charmed baryon( $m_s = 174\text{MeV}$ )	-8.49	4.53	2.93	-1.21	-0.37	0.26
Bottom baryon( $m_s = 166\text{MeV}$ )	-8.49	4.53	2.93	-1.16	-0.35	0.25
Yang <i>et al.</i> [35]	$-10.08 \pm 0.24$	$4.15 \pm 0.93$	$8.54 \pm 0.86$	$-2.53 \pm 0.14$	$-3.29 \pm 0.57$	$-1.34 \pm 0.56$